WSI Applied Remote Sensing and Analysis

March 19, 2013

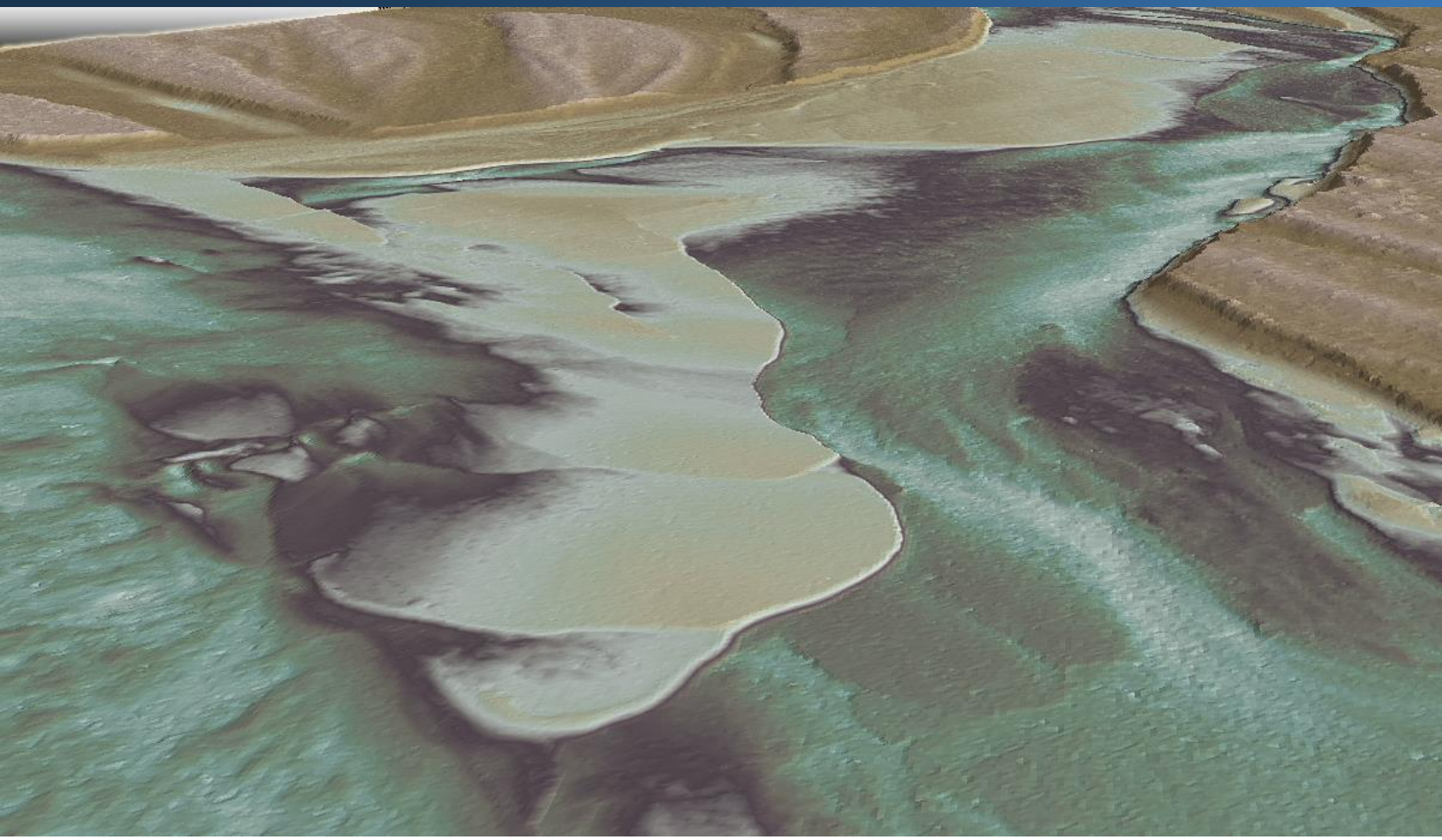

Sandy River LiDAR

Technical Data Report

DOGAMI
800 NE Oregon St. #28, Suite 965
Portland, OR 97232
PH: 971-673-1555

WSI Corvallis Office
517 SW 2nd St., Suite 400
Corvallis, OR 97333
PH: 541-752-1204

TABLE OF CONTENTS

Cover Photo: Gridded bathymetric returns from green LiDAR. The bare-earth model is colored by elevation.

INTRODUCTION

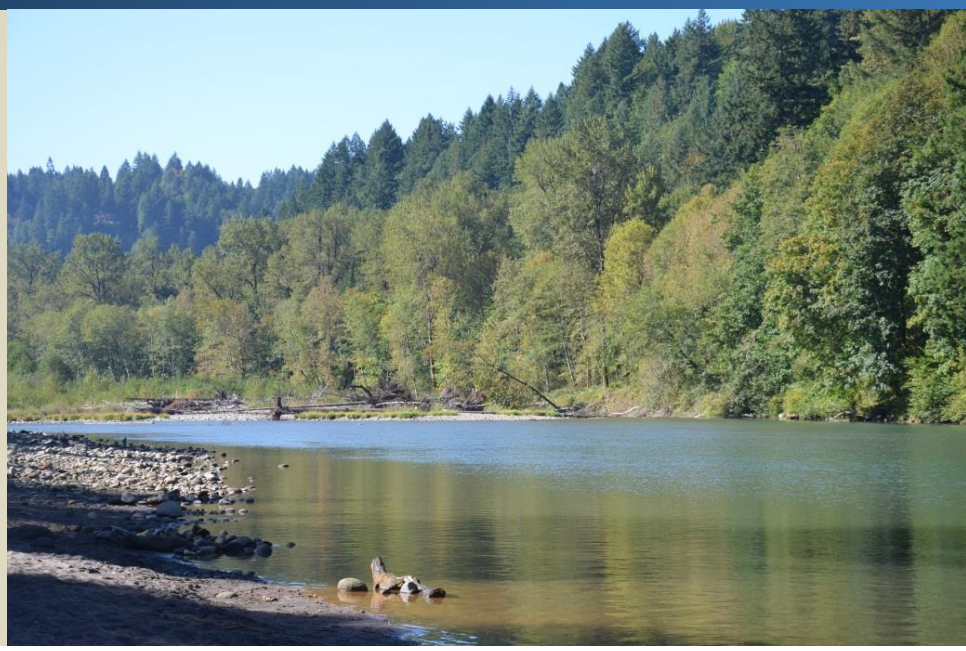

View of the Sandy River, Oregon looking downstream from the Oxbow Park boat launch

In July 2012, Watershed Sciences, Inc. (WSI) was contracted by the Oregon Department of Geology and Mineral Industries (DOGAMI) to collect airborne topo-bathymetric LiDAR (Light Detection and Ranging) data for the Sandy River, Oregon. The data were collected to map channel and floodplain morphology and to evaluate the effectiveness of new topo-bathymetric LiDAR technology in a Pacific Northwest riverine environment. The project was conducted through the Oregon LiDAR Consortium (OLC) with contributions from DOGAMI, the Federal Emergency Management Agency (FEMA), and the Bureau of Land Management (BLM).

The Sandy River flows through areas of steep terrain and dense tree canopy and is home to Chinook and Coho salmon and Steelhead trout. The Sandy River is further distinguished by the 2007 removal of the Marmot Dam (river mile 30) and has been the focus of ongoing monitoring to understand the impacts of dam removal on downstream morphology and fish habitat. The nature of the river makes it challenging for traditional transect or boat-based bathymetric surveys.

WSI collected the airborne topo-bathymetric data, calibrated the points, and created all final deliverables. WSI partnered with Dewberry & Davis, LLC[1] who corrected and classified the sub-surface returns. WSI also collected and processed traditional (near infrared wavelength) LiDAR and natural color digital imagery simultaneous with the topo-bathymetric LiDAR (green wavelength). The traditional LiDAR provides a comparison to the topo-bathymetric data while the digital imagery provided a reference for water conditions at the time of the survey.

This report accompanies the delivered data products and documents acquisition procedures, processing methods, and results of all accuracy assessments. This documentation also covers the near infrared

[1] Dewberry & Davis, LLC, 1000 N. Ashley Dr., Suite 801, Tampa, FL 33602

(NIR) LiDAR data and three-band orthoimagery collected at the time of the bathymetric LiDAR acquisition. Project specifics are shown in Table 1, the project extent can be seen in Figure 1, and a complete list of contracted deliverables provided to DOGAMI can be found in Table 2.

Table 1: Acquisition date, acreage, and data types collected for the Sandy River

Project Site	Contracted Acres	Acquisition Dates	Data Type
Sandy River	6,923	09/22/2012	Green LiDAR
			NIR LiDAR
			3 band (RGB) Digital Imagery

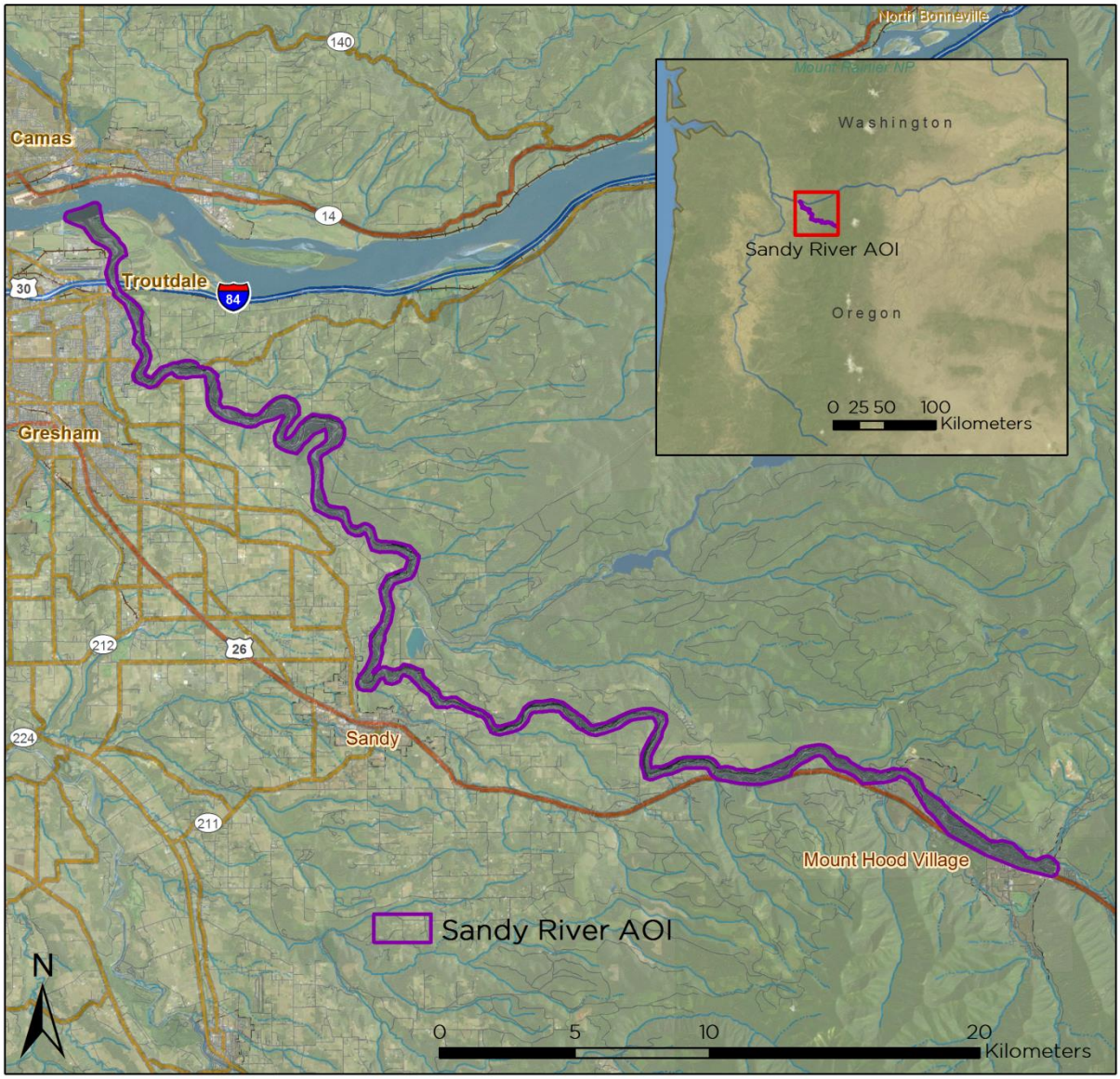

Figure 1: Location map of the Sandy River LiDAR site in Oregon

Table 2: Products delivered to DOGAMI for the Sandy River LiDAR site

Projection: UTM Zone 10 North Horizontal Datum: NAD83 (CORS96) Vertical Datum: NAVD88 (GEOID09) Units: Meters	
Topobathymetric LiDAR	
LAS Files	All Returns (LAS v 1.2)
Rasters	1-meter ESRI Grids and GeoTiffs • Combined Topo-bathymetric Model • Water depth model 0.5-meter GeoTiffs • Intensity Images
Vectors	Shapefiles (*.shp) • Site Boundary • LiDAR Index • DEM/DSM Index • Water's edge 3D polyline • Confidence layer for topobathy model
Near-infrared LiDAR (Supplementary)	
LAS Files	All Returns (LAS v. 1.2)
Rasters	1-meter ESRI Grids and GeoTiffs • Bare Earth Model • Highest Hit Model 0.5-meter GeoTiffs • Intensity Images
Vectors	Shapefiles (*.shp) • Site Boundary • LiDAR Index • DEM/DSM Index
Digital Imagery (Supplementary)	
Orthophotos	3-band Imagery Mosaics (7-cm GeoTIFFs)
Vectors	Shapefiles (*.shp) • Orthoimagery Index

Riegl VQ-820-G topo-bathymetric LiDAR sensor installation in WSI's Cessna Caravan

Instrumentation

Shallow water, airborne topo-bathymetric LiDAR is a relatively new discipline with several commercial sensors entering the market within the past year. These systems vary widely in technical specifications and few have been thoroughly tested in the riverine environments of the mountain west. For this project, WSI deployed the Riegl VQ-820-G system, introduced in 2012, which features high pulse density, short pulse widths, and narrow beam divergence. The specifications of this system made it very promising for mapping river channels with highly variable elevations and channel widths. The system has demonstrated hydrographic depth ranging capability to 1 secchi depth, but its full capabilities for different inland water regimes are still being explored. The Sandy River project is one of the first rigorous tests completed with this system. The sensor was installed in the forward camera port in WSI's Cessna Caravan, and the airborne surveys were conducted in cooperation with Riegl USA.

The NIR LiDAR data was collected with a Leica ALS60 and natural color digital imagery was collected using a Leica RCD150 (39 MP) camera. The Leica ALS60 and the digital camera were installed in the aft camera port. The installation configuration allowed simultaneous collection of the topo-bathymetric data, near infrared data, and digital imagery. The NIR LiDAR provided data for comparison to the topo-bathymetric surface and a second wavelength (1,064 nm) for potential research into the advantages of multi-wavelength LiDAR in a river floodplain. The digital imagery provided a reference for water conditions and clarity within the river. The collection and processing of the NIR LiDAR and digital imagery are discussed in later chapters.

Planning

The airborne survey was designed to collect a point density of 4-5 pulses/m^2 for the topo-bathymetric LiDAR. The flight was planned with a scan angle of ±20^o and 50% side-lap. The 50% side-lap was used to ensure uniform coverage and to minimize laser shadowing due to vegetation and terrain. The flights were conducted in the late fall during base flow conditions to maximize water clarity and ensure shallow depths (Figure 2).

The flight lines were developed using ALTM-NAV Planner (v.3.0) software and Leica Mission Pro Flight Planning and Evaluation (FPES) software. Efforts were taken to optimize flight paths by minimizing flight times while meeting all accuracy specifications. The WSI acquisition staff considered all factors such as air space restrictions, private property access, and GPS quality in the planning of this mission.

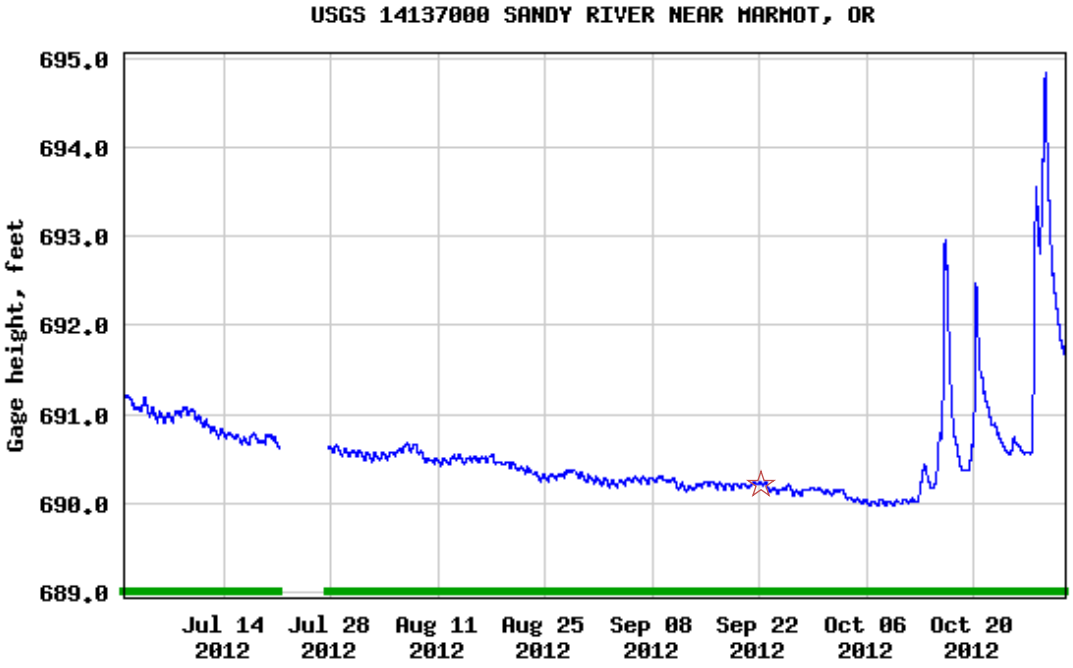

Figure 2: Flow conditions on the Sandy River at the time of the LiDAR acquisition

Airborne LiDAR Survey

The Riegl VQ-820-G uses a green-wavelength (μ = 532 nm) laser that, in addition to collecting vegetation and topography data, is able to penetrate the water surface with the 532-nm wavelength which provides for minimal spectral absorption. The sensor also collects both discrete returns (similar to the NIR data) and full-waveform data (every other pulse) for more rigorous feature extraction and evaluation of point returns. The recorded waveform enables range measurements for all discernible targets for a given pulse. The typical number of returns digitized from a single pulse ranged from 1 to 7 for the Sandy River project area.

The Leica ALS60 uses a NIR wavelength (μ =1,064nm) laser that has been proven to provide high value terrestrial topography data. The NIR wavelengths do not penetrate the water column and thus provide water surface returns for received pulses off of water surface. The Leica system collects 8-bit intensity information and does not store waveform information. Table 3 summarizes the settings used to yield an average pulse density of 4-5 pulses/m^2 for the topo-bathymetric LiDAR and ≥8 pulses/m^2 for the NIR LiDAR.

Table 3: Survey settings and specifications for the Sandy River LiDAR

LiDAR Survey Settings & Specifications		
Sensor	Riegl VQ820G	Leica ALS60
Survey Altitude (AGL)	600 m	600 m
Target Pulse Rate	130 kHz	135 kHz
Laser Wave Length	532nm	1064 nm
Laser Pulse Diameter	60cm	15 cm
Scan Pattern	Elliptical	Sinusoidal
Field of View	40°, 20° forward fixed angle	40°
GPS Baselines	≤13 nm	≤13 nm
GPS PDOP	≤3.0	≤3.0
GPS Satellite Constellation	≥6	≥6
Maximum Returns	unlimited	4
Intensity	16-bit	8-bit
Full Waveform	Yes	No
Resolution/Density	4-5 pulses/m^2	Average 8 pulses/m^2

To accurately solve for laser point position (geographic coordinates x, y, and z), the positional coordinates of the airborne sensor and the attitude of the aircraft were recorded continuously throughout the LiDAR data collection mission. Position of the aircraft was measured twice per second (2 Hz) by an onboard differential GPS unit. Aircraft attitude was measured 200 times per second (200 Hz)

as pitch, roll, and yaw (heading) from an onboard inertial measurement unit (IMU). To allow for post-processing correction and calibration, aircraft/sensor position and attitude data are indexed by GPS time.

Ground Survey

Ground survey data is used to geospatially correct the aircraft positional coordinate data and to perform quality assurance checks on final LiDAR data and orthoimagery products. Ground professionals set permanent survey monuments and collect real time kinematic (RTK) surveys to support the airborne LiDAR acquisition process.

Monumentation

The spatial configuration of ground survey monuments provided redundant control within 13 nautical miles of the mission areas for LiDAR flights. Monuments were also used for collection of ground control points using RTK survey techniques (see **RTK** below).

Monument locations were selected with consideration for satellite visibility, field crew safety, and optimal location for RTK coverage. WSI established 2 new monuments for the Sandy River LiDAR project (Table 4, Figure 3). New monumentation was set using 5/8”x30” rebar topped with stamped 2" aluminum caps. WSI’s professional land surveyor, Chris Yotter-Brown (OR PLS #60438LS) oversaw and certified the establishment of monuments.

Table 4: Monuments established for the Sandy River LiDAR acquisition. Coordinates are on the NAD83 (CORS96) datum, epoch 2002.00.

Monument ID	Latitude	Longitude	Ellipsoid (meters)
SANDY_03	45° 23’ 11.51760”	-122° 14’ 05.13779”	338.515
SANDY_04	45° 22’ 42.70869”	-122° 13’ 34.31097”	344.345

To correct the continuous onboard measurements of the aircraft position recorded throughout the missions, WSI concurrently conducted multiple static Global Navigation Satellite System (GNSS) ground surveys (1 Hz recording frequency) over each monument. After the airborne survey, the static GPS data were triangulated with nearby Continuously Operating Reference Stations (CORS) using the Online Positioning User Service (OPUS[2]) for precise positioning. Multiple independent sessions over the same monument were processed to confirm antenna height measurements and to refine position accuracy.

[2] OPUS is a free service provided by the National Geodetic Survey to process corrected monument positions. http://www.ngs.noaa.gov/OPUS

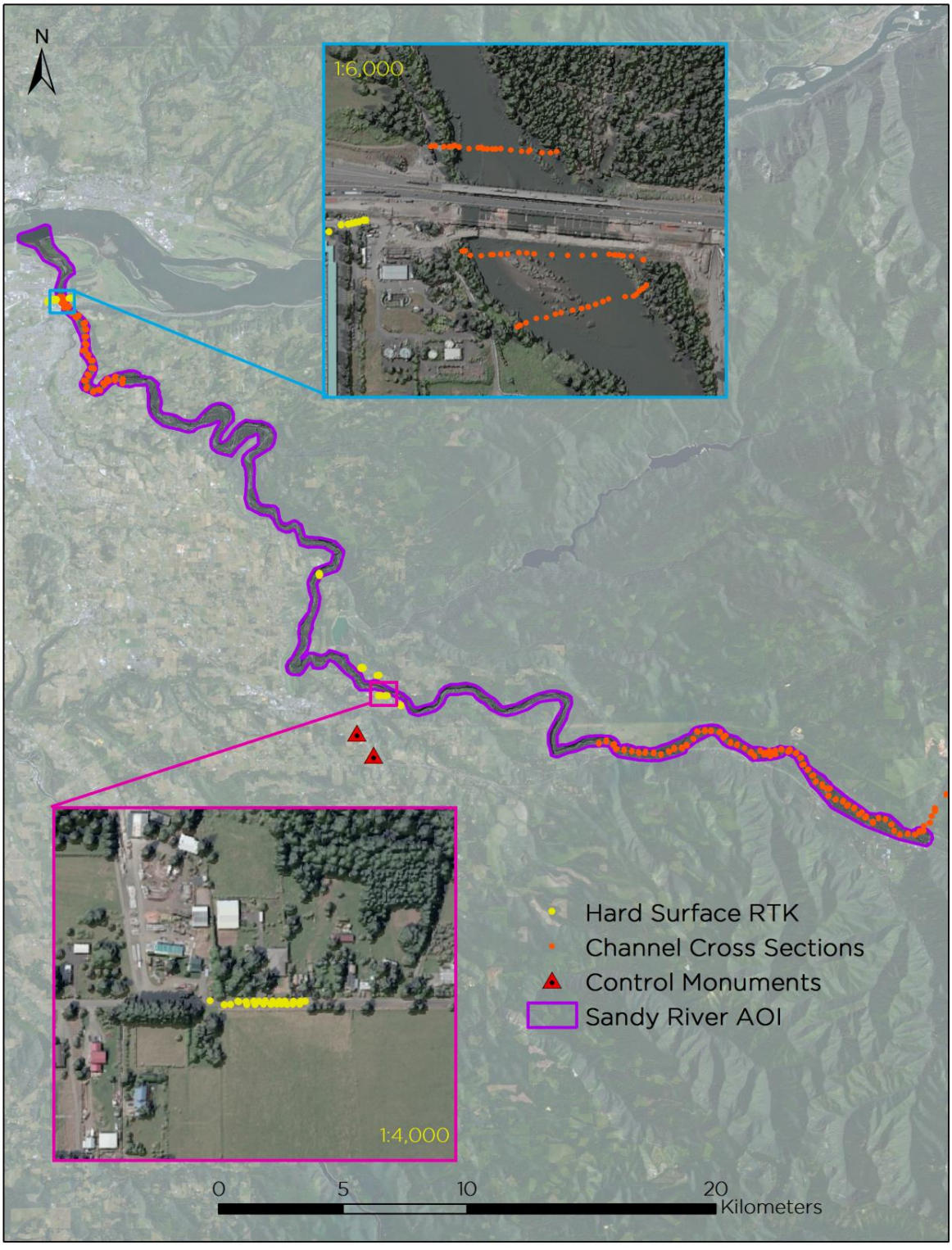

Figure 3: Monument and RTK checkpoint location map including bathymetric RTK locations collected by Atkins Geomatics

Monuments were established according to the national standard for geodetic control networks, as specified in the Federal Geographic Data Committee Draft Geospatial Position Accuracy Standards, Part 2, Table 2.1 (FGDC-STD-007.2-1998). This standard provides guidelines for classification of monument quality at the 95% confidence interval. The monument rating for this project can be seen in Table 5.

Table 5: Federal Geographic Data Committee monument rating

Direction	Rating
St Dev $_{NE}$:	0.010 m
St Dev $_{z}$:	0.020 m

Ground Check Points

Ground check points were collected using real time kinetic (RTK) survey techniques. A Trimble R7 base unit was positioned at a nearby monument to broadcast a kinematic correction to a roving Trimble R8 GNSS receiver. All RTK measurements were made during periods with a Position Dilution of Precision (PDOP) of ≤ 3.0 with at least six satellites in view of the stationary and roving receivers. When collecting RTK data, the rover would record data while stationary for five seconds, then calculate the pseudo range position using at least three one-second epochs. Relative errors for the position must be less than 1.5 cm horizontal and 2.0 cm vertical in order to be accepted.

RTK positions were collected on paved roads that had good satellite visibility. RTK measurements were not taken on highly reflective surfaces such as center line stripes or lane markings on roads due to the increased noise seen in the laser returns over these surfaces. The distribution of RTK points depended on ground access constraints and may not be equally distributed throughout the study area.

All static surveys were collected with Trimble model R7 GNSS receivers equipped with a Zephyr Geodetic Model 2 RoHS antenna. A Trimble model R8 GNSS receiver was used to collect RTK. All GNSS measurements were made with dual frequency L1-L2 receivers with carrier-phase correction (Table 6).

Table 6: Trimble equipment identification

Receiver Model	Antenna	OPUS Antenna ID	Use
Trimble R7 GNSS	Zephyr GNSS Geodetic Model 2	TRM57971.00	Static
Trimble R8	Integrated Antenna R8 Model 2	TRM_R8_GNSS	RTK

Channel Cross Sections

Channel cross sections were surveyed within the LiDAR project area by Atkins Geomatics in an effort to gather bottom elevations in the Sandy River as part of a larger flood hazard study of the Sandy River Watershed. DOGAMI provided these data to WSI to help evaluate the resolution and accuracy of the bathymetric LiDAR returns. The LiDAR data was originally calibrated to bare earth RTK check points collected by WSI; however, during processing, all points falling below the water surface undergo a refraction transformation. The cross section data provided a method of quantifying the success of the refraction process and accuracy of the submerged topography classification. Atkins Geomatics' Project Narrative in included as Appendix A. Figure 3 shows the distribution of channel cross sections in this project.

As indicated in the Atkins Geomatics report, collecting in-channel transects with field based RTK surveying methods has several limitations including safety concerns and technical issues. Access points to the river are limited due to steep banks, high water velocity, and private property concerns. Additionally, the Sandy River is heavily vegetated on many of its banks with both deciduous and coniferous trees. This results in no substantial "leaf-off" time period thus limiting GPS satellite visibility in certain areas which can reduce survey accuracy. In some cases, GPS RTK methods were supplemented with tape and hand level measurements (Appendix A).

While it is useful to have this supplemental dataset for accuracy reporting, the discreet nature of transects as well as the logistical issues of collecting the data highlight the importance of continuous remotely collected bathymetric data. Two sections of Sandy River transect data were provided to WSI. They were separated by 27 river miles and collected one month before (08/30/12) and after (10/22/12) the bathymetric LiDAR flight (09/22/12). This temporal difference is important to recognize when comparing transect data to the bathymetric LiDAR data. The Sandy River is a highly dynamic system with frequent sediment transport. This constantly changing system highlights the importance of capturing data with minimal temporal difference. A major benefit of the bathymetric LiDAR is the ability to capture larger study areas in hours to provide a "snapshot" of a highly dynamic system, as compared to days using traditional techniques.

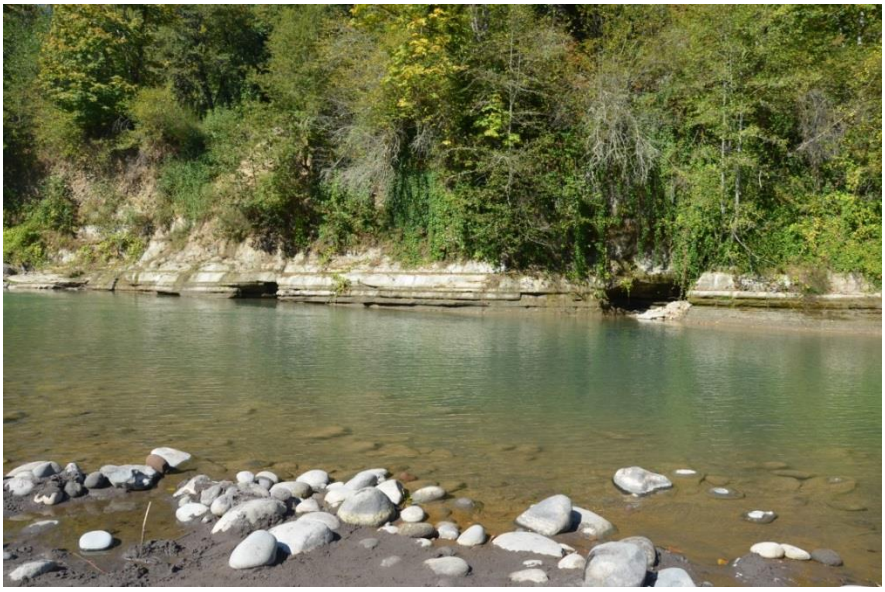

Bathymetric LiDAR Data

Prior to the mission, a boresight calibration flight was conducted in Corvallis, OR and processed by WSI to ensure accurate initial sensor alignment. An individual mission calibration was also performed on the Sandy River data set using Riegl's RiProcess software. RiProcess was then used by WSI to further refine line-to-line calibration of the topo-bathymetric LiDAR dataset to match collected hard surface RTK control points.

Upon completion of calibration, Dewberry processed the LiDAR returns with a combination of manual and automated techniques using both the Riegl software and in-house proprietary software to differentiate the bathymetric and terrestrial data. WSI processed NIR LiDAR and the orthorectified digital imagery, which were also used to facilitate the processing of the bathymetric returns. Once bathymetric points were differentiated, they were spatially corrected for refraction through the water column based on the angle of incidence of the laser. Dewberry refracted water column points and classified the resulting point cloud. The resulting data was sent back to WSI for further review and product creation. Figure 4 shows the various datasets used in the bathymetric analysis while Table 7 summarizes the steps used to process the bathymetric LiDAR data.

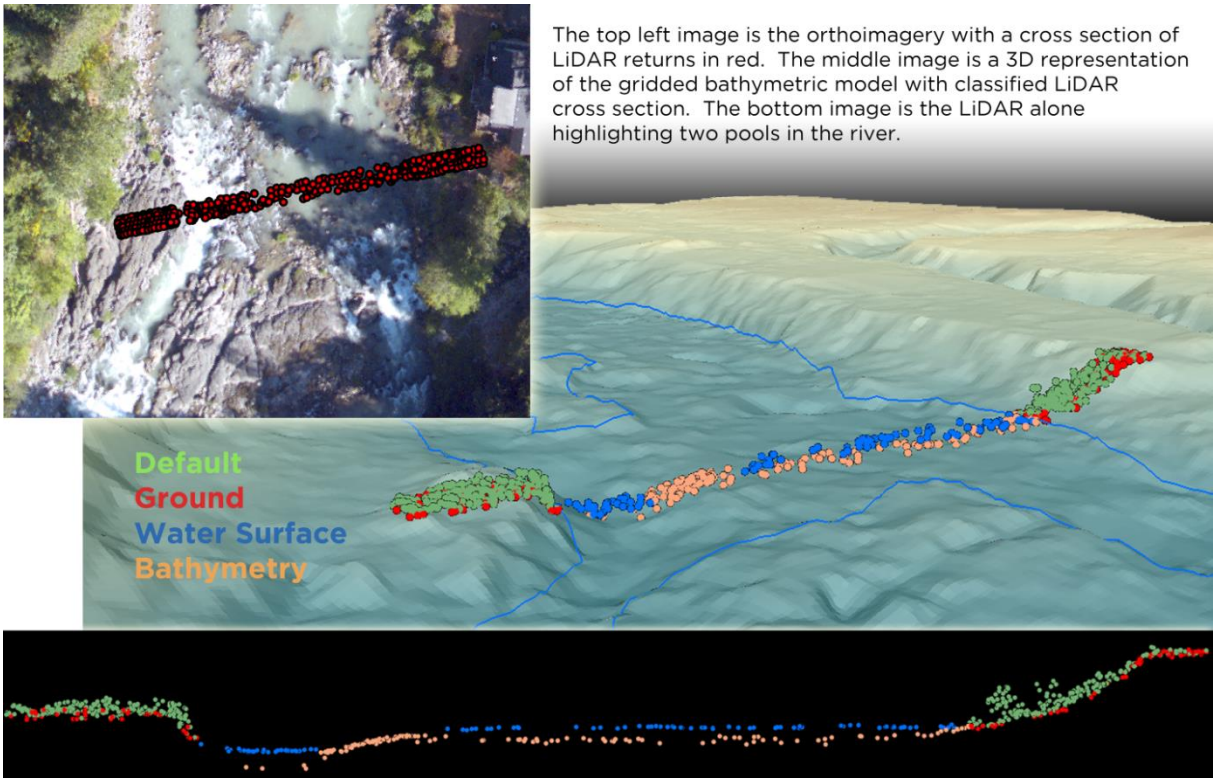

Figure 4:Example of the imagery and data sets used in the Sandy River Bathymetric analysis

Table 7: Bathymetry LiDAR processing workflow

Bathymetric LiDAR Processing Step	Software Used
Resolve kinematic corrections for aircraft position data using kinematic aircraft GPS and static ground GPS data.	Waypoint GPS v.8.3 Trimble Business Center v.2.80 Blue Marble Desktop v.2.5
Develop a smoothed best estimate of trajectory (SBET) file that blends post-processed aircraft position with attitude data. Sensor head position and attitude are calculated throughout the survey. The SBET data are used extensively for laser point processing.	PosPac MMS 6.1
Calculate laser point position by associating SBET position to each laser point return time, scan angle, intensity, etc. Create raw laser point cloud data for the entire survey in Riegl data format.	RiProcess v.1.5.7.128
Filter erroneous points.	RiProcess v.1.5.7.128
Perform automated line-to-line calibrations for system attitude parameters (pitch, roll, heading), mirror flex (scale) and GPS/IMU drift. Calibrations are calculated on matching surfaces within and between each line and results are applied to all points in a flight line. Every flight line is used for relative accuracy calibration.	RiProcess v.1.5.7.128
Assess statistical absolute accuracy via direct comparisons of surface points to ground RTK survey data. Data are exported to standard LAS 1.2 or 1.3 formats.	RiProcess v.1.5.7.128
Generate a water's edge line from the NIR data.	Dewberry LiDAR Processor (DLP)
Classify points falling within the water's edge line as water and apply a refraction correction.	DLP
Use full waveform data to analyze water surface, bathymetry, and water column returns.	DLP
Generate topo-bathymetric models as triangulated surface.	TerraScan v.12.004 ArcMap v. 10.1 TerraModeler v.12.002

Point Classification

As with standard NIR LiDAR data, bathymetric (green) LiDAR returns are classified into categories according to whether the points are considered above ground, ground, or water. Additional LiDAR classifications were created for bathymetric processing by adding categories for channel bottom, water surface, and water column points (Table 8,Figure 5).

Table 8: WSI/Dewberry LAS classificaion standards applied to bathymetric LiDAR dataset

Classification Number	Classification Name	Classification Description
1	Default	Laser returns that are not included in the ground classification.
2	Ground	Ground that is determined by a number of automated and manual cleaning algorithms to determine the best ground model the data can support.
19	Channel Bottom	Ground points that fall within the water's edge breakline which characterize the submerged topography.
20	Water Surface	Default points that fall within the water's edge breakline which characterize the surface of the water.
24	Water Column	Any remaining points within the water's edge breakline that do not represent the water surface or bathymetry.

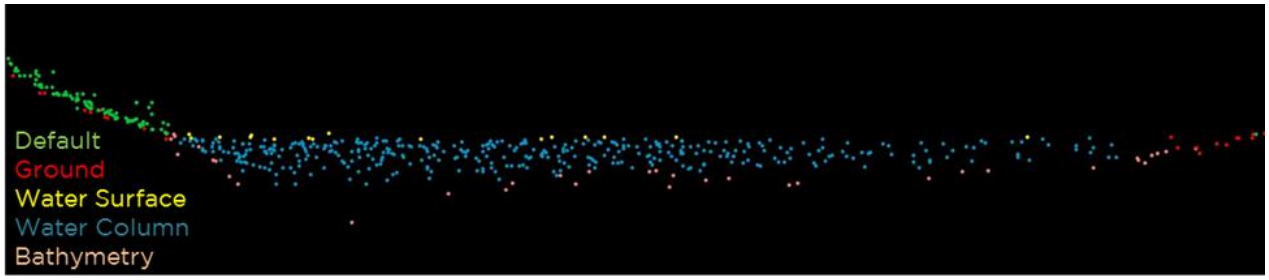

Figure 5: Sample bathymetric LiDAR transect classification

Full Waveform Processing

Initial echo analysis is accomplished with Riegl's online waveform processing. In online waveform processing, discrete returns are digitized from the echo signal based on the amplitude and pulse deviation of returning energy. To facilitate discrimination of ground points versus water column points and bathymetry points, the Riegl VQ-820-G uses the online waveform processing system that generates a discrete point cloud dataset at time of capture ("online") from the full waveform signal. The system also records geo-referenced waveforms for a subsample of the data (configured for every other pulse). The waveforms are used in determining accurate bathymetry in shallow submerged environments. The separation of the water surface and bottom return in shallow depths requires further analysis and customized methods to 'decompose' or 'deconvolve' the waveform (Figure 6).

Furthermore, certain parameters such as attenuation coefficients need to be set when processing data in various depth ranges and water column parameters. Information derived from the waveforms is used to set these parameters. The determination of the bottom return also needs to be corrected for the change in speed of light through the water column and the refraction of light at the air/water interface. The processed waveforms are used to validate the online digitization of the initial point cloud data.

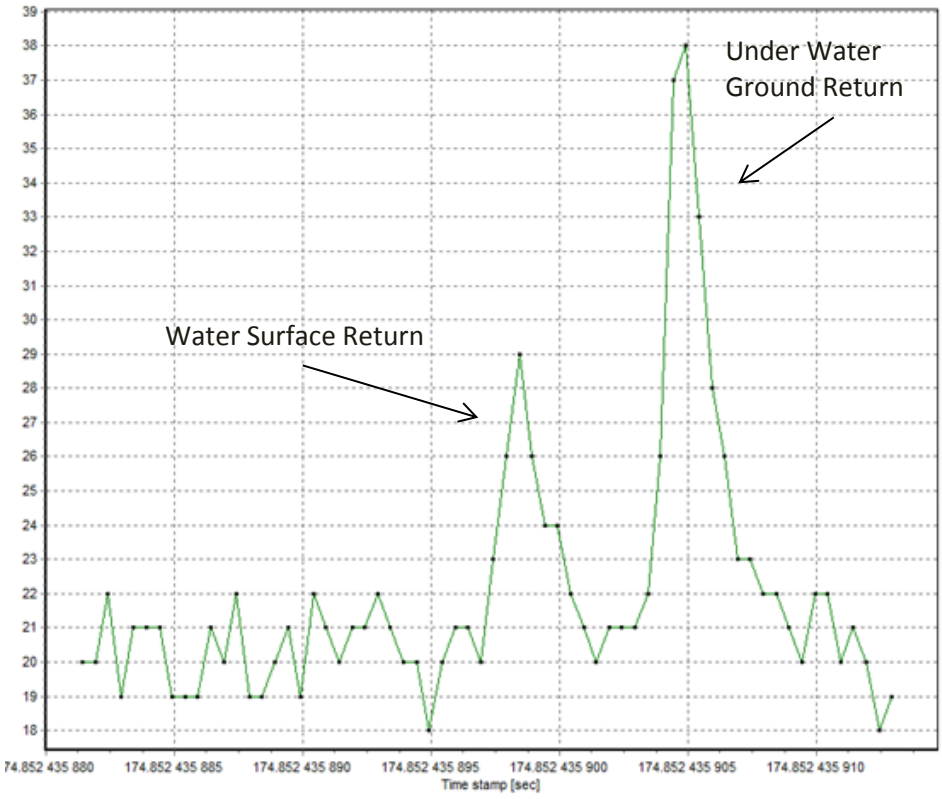

Figure 6: Sample Riegl VQ-820-G bathymetry waveform showing a distinct surface and bottom return from the Sandy River

Ground level image looking downstream from Dodge Park, near the town of Sandy, OR. The Sandy River is characterized by occasional deep pools connected by shallow riffles and runs.

Bathymetric LiDAR

In order to determine accuracy and completeness of the bathymetric surface, several parameters were considered: depth penetration below the water surface, return density, and spatial accuracy.

Depth Penetration

Secchi depth is a qualitative measure of the transparency of the water. The transparency of water affects how deep light (in this case, the green 532-nm laser) will penetrate below the surface and is related to turbidity. The specified depth penetration range of the Riegl VQ-820-G sensor is one Secchi depth. A single Secchi depth measurement of 2.1 m was made at a deep pool near the Oxbow Park Boat Launch (Figure 7). Several attempts were made to measure Secchi depths at additional access locations, but the river at these locations was shallow and did not exceed one Secchi depth. The Sandy River is least turbid during the fall months and based on visual observations, the single measurement was considered to be representative of the turbidity of the surveyed reach.

Sampled Secchi Depth	
Latitude	45° 29’ 50.97” N
Longitude	-122° 17’ 36.55” W
Secchi Depth	2.1 m
Pool Depth	3.99 m

Figure 7: Pool at Oxbow Park where a Secchi depth measurement of 2.1 m was recorded.

The resulting Secchi depth provides a predictive indicator of the depth capabilities of the bathymetric LiDAR on the Sandy River. In order to assess the actual depth penetration of the bathymetric LiDAR throughout the project study area, a model of the bathymetry bottom classified points was then subtracted from the water surface model derived from the NIR LiDAR. The distribution of resulting water column depths reflect the shallow nature of the river with the majority of the depths being 1 meter or less, well under the 1-Secchi depth limitation of the sensor (Figure 8 and Figure 9).

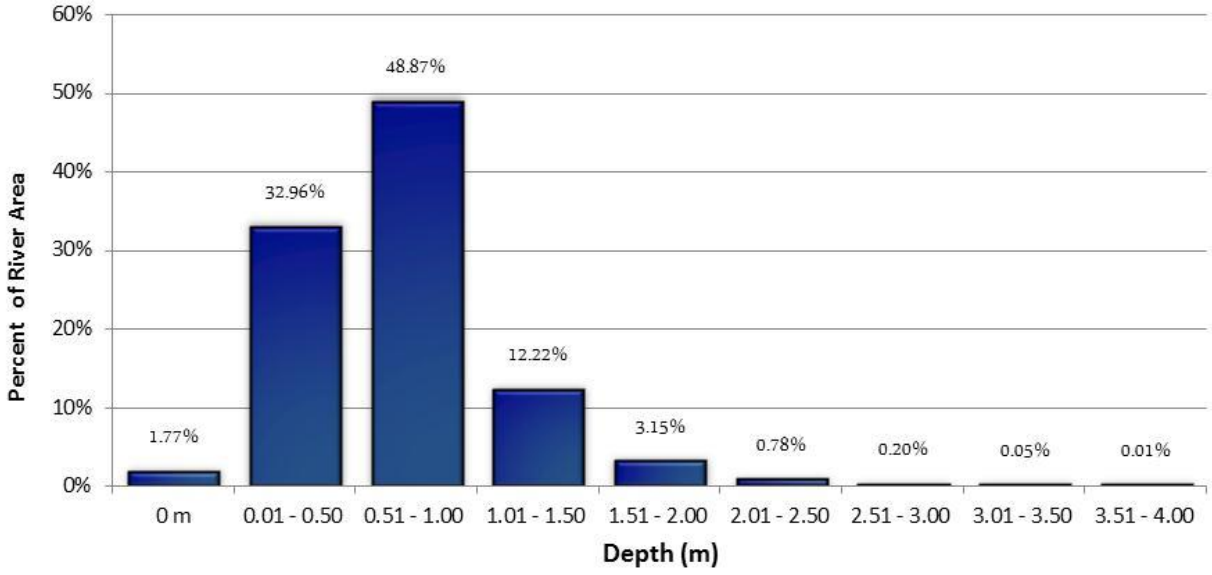

Figure 8: Bathymetric depth measurement ranges calculated through the survey area

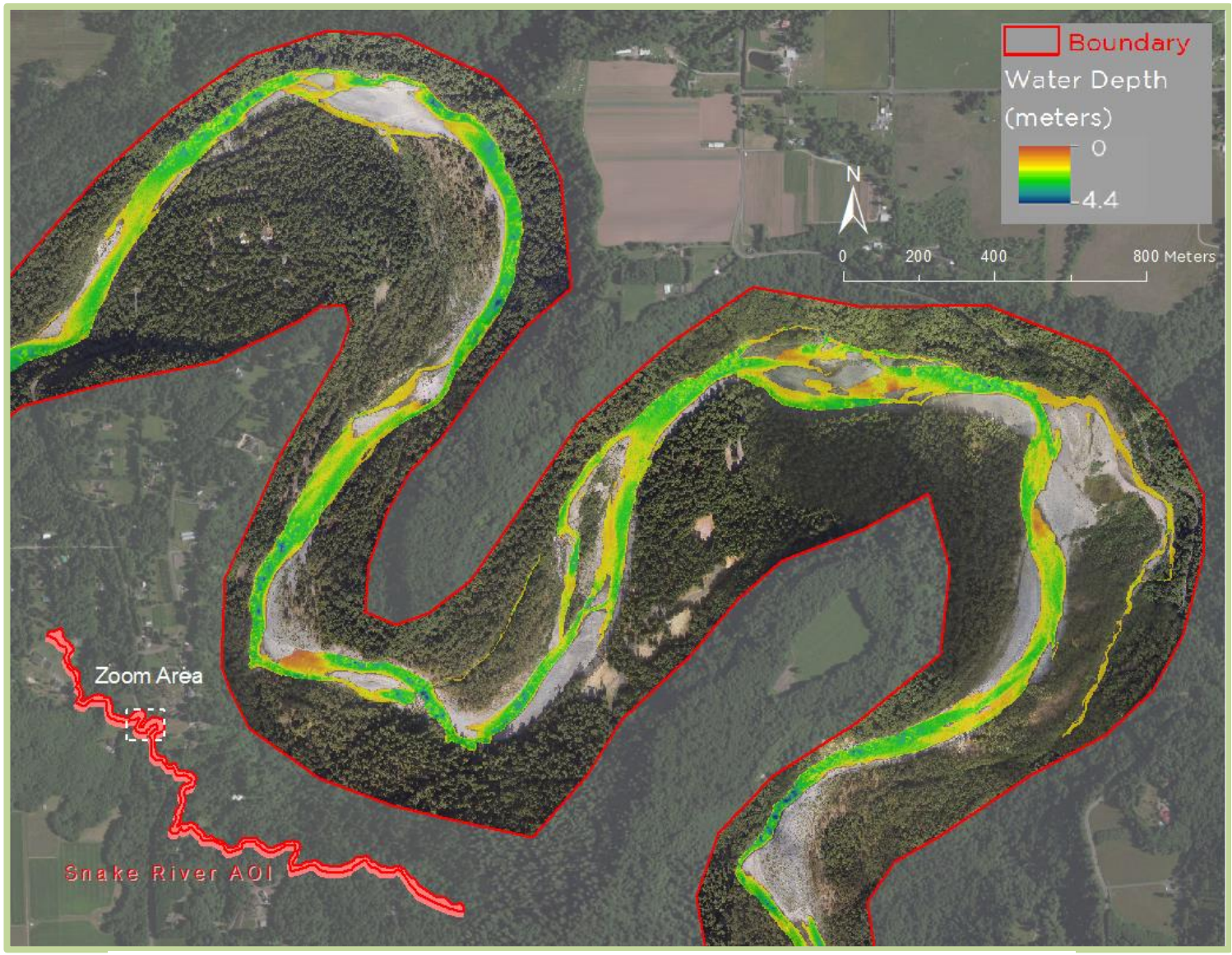

Figure 9: Water depth model of a reach along the Sandy River, Oregon

Bathymetric LiDAR Density

The average first-return (native) density for the bathymetric LiDAR data was 6.3 points/m^2 (Table 9). The average density for underwater bottom returns was 1.6 points/m^2 (Figure 10). The statistical and spatial distribution of first returns (Figure 11 and Figure 13) and classified topo-bathymetric returns (Figure 12 and Figure 14) are portrayed below. Usual factors affecting terrestrial ground classified returns include the laser's ability to penetrate vegetation, while bathymetric bottom classified returns are limited by turbidity and depth.

Table 9: Average Green LiDAR point densities

Classification	Point Density
First-Return	6.3 points/m^2
Ground Classified	0.9 points/m^2
Bathymetry	1.6 points/m^2

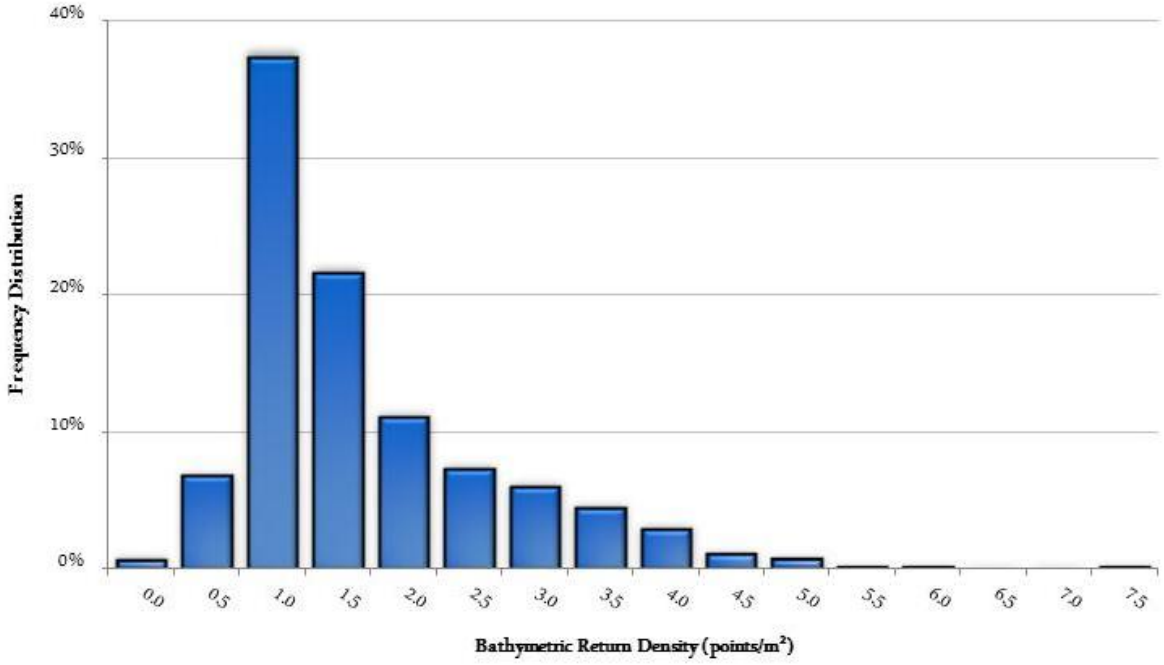

Figure 10: Frequency distribution of bathymetric bottom return density of a 100m^2 gridded sample area

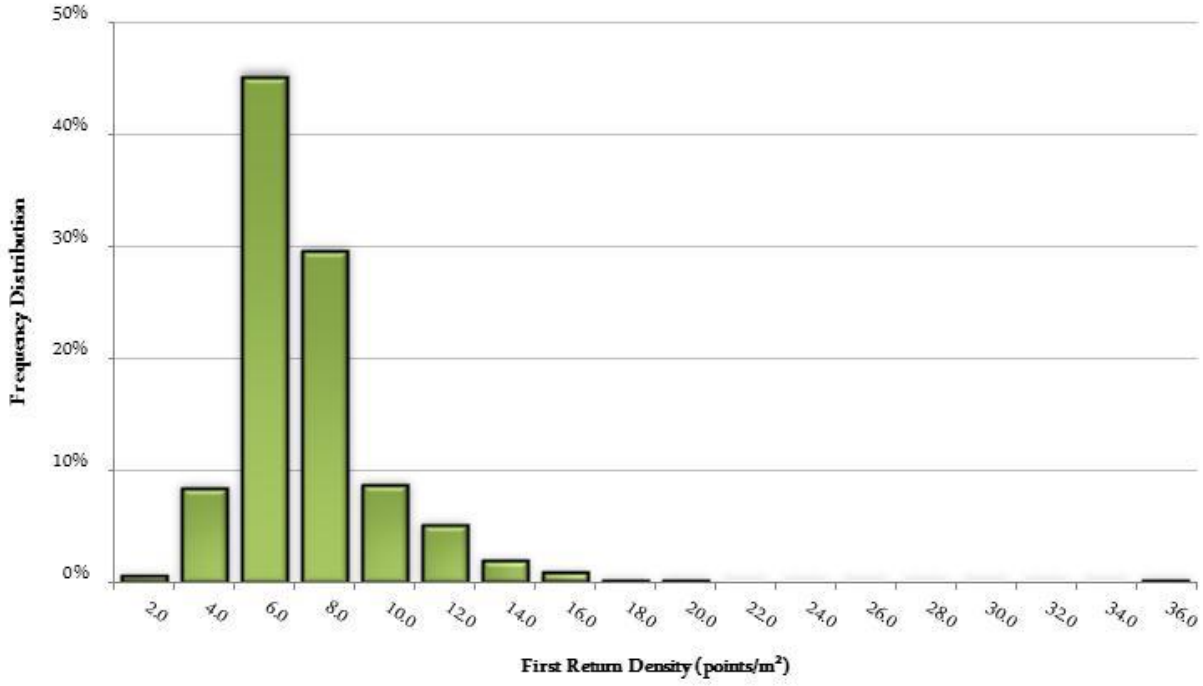

Figure 11: Frequency distribution of first return (native) density of a 100m^2 gridded sample area

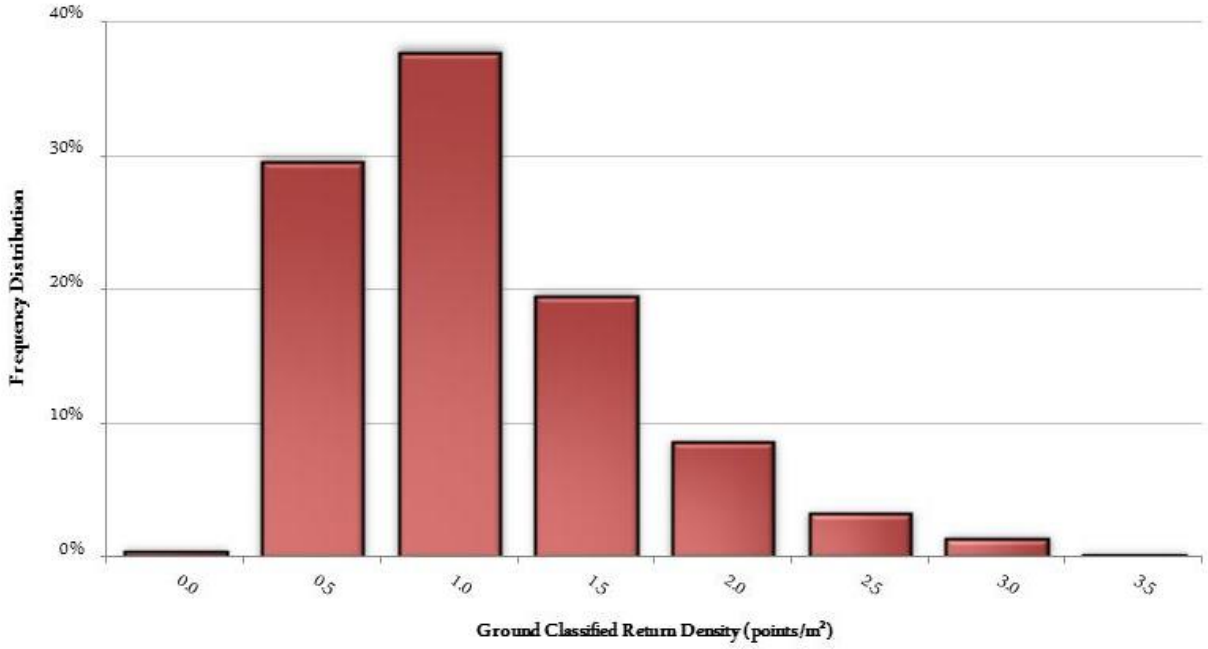

Figure 12: Frequency distribution of ground classified return density of a 100m^2 gridded sample area

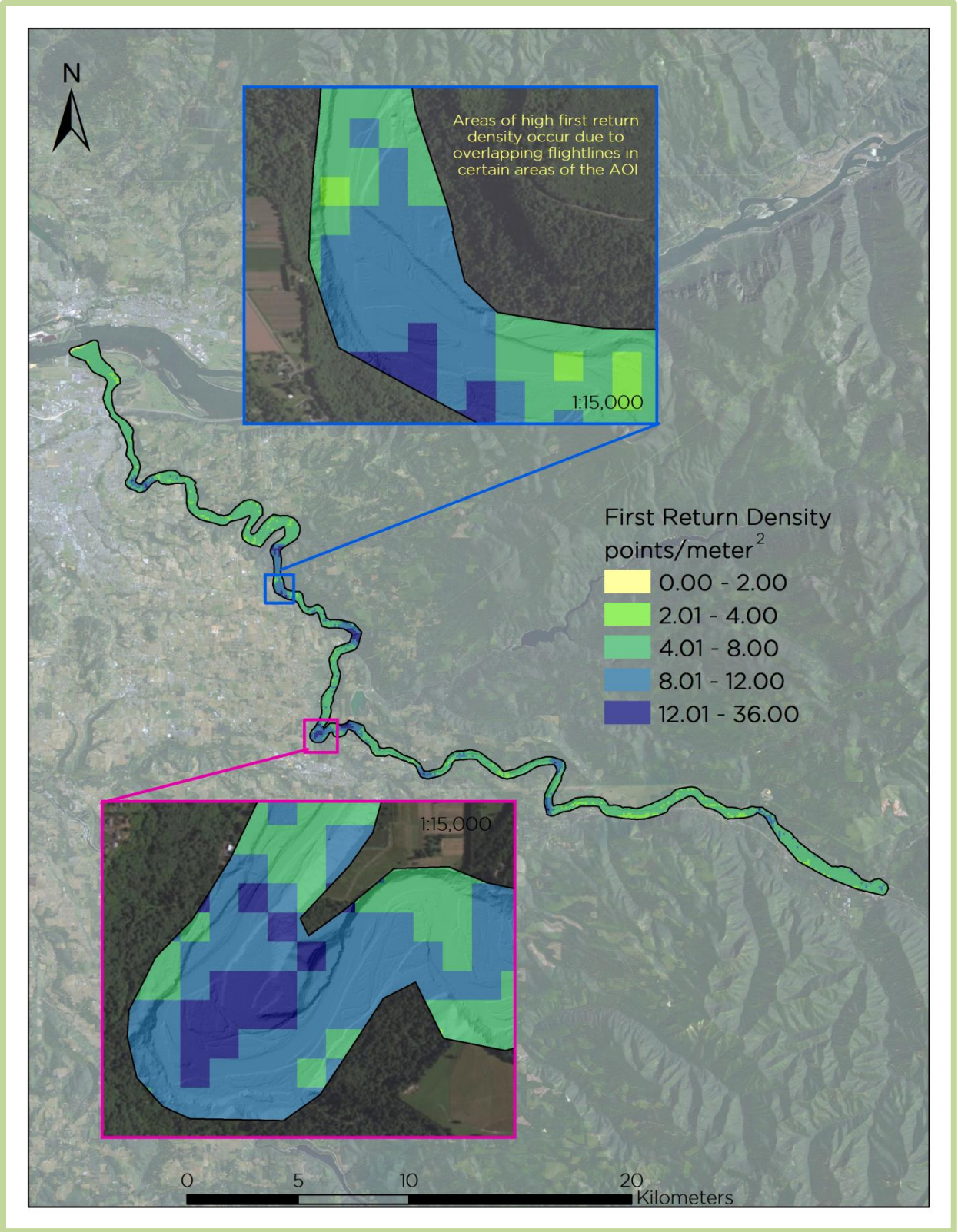

Figure 13: Native density map for the Sandy River LiDAR site

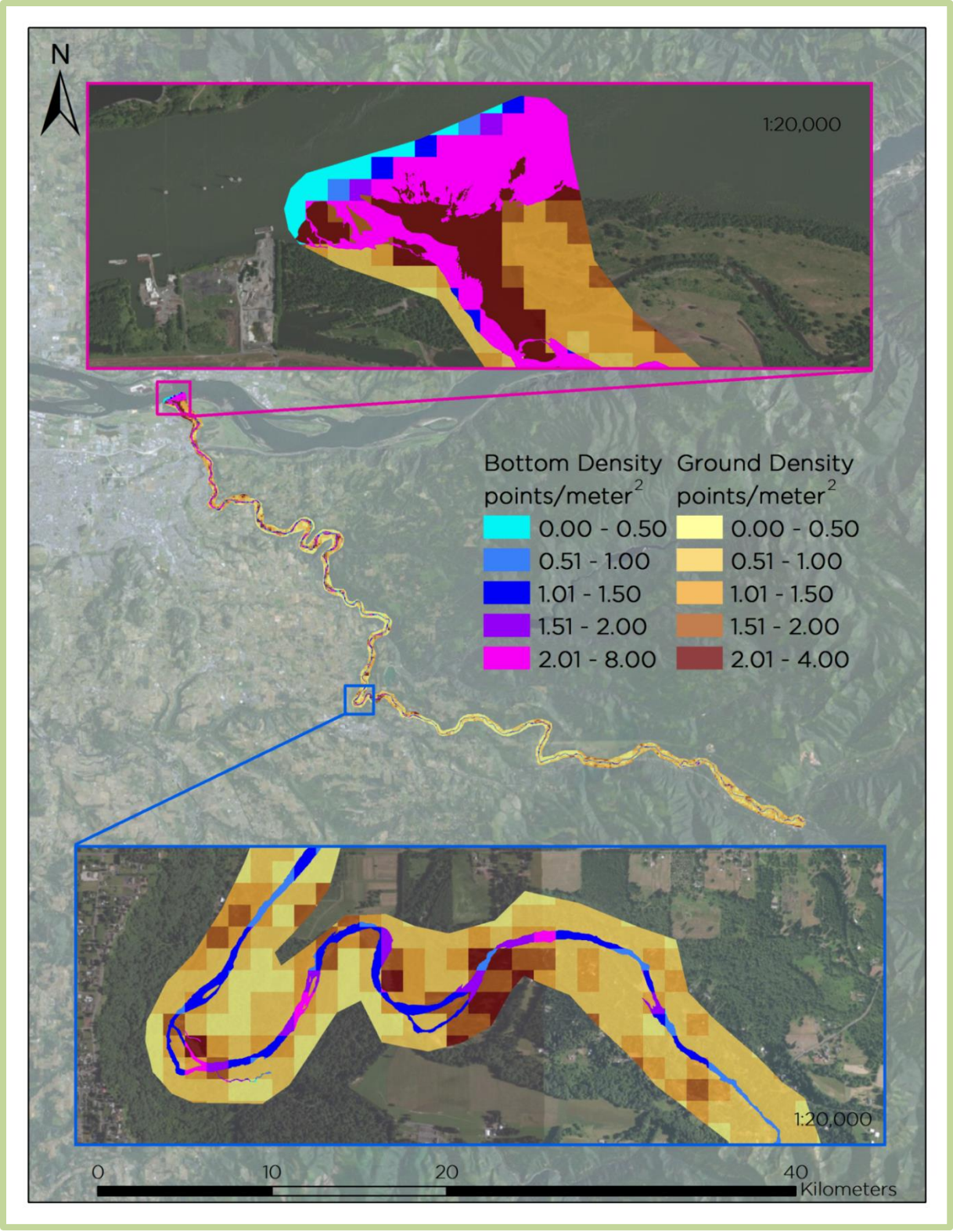

Figure 14: Topo-bathymetric density map for the Sandy River LiDAR site. The density of bathymetric bottom returns is seen dropping off at the mouth of the Sandy River at the confluence with the deeper Columbia River.

The distribution of the point density within the river channel varied depending on depth. Confidence in bathymetric elevation data was assessed by looking at point density within an area of 15 m2 radiating out from the center of any given 1-m2cell (r=2.19 m). Areas resulting in a point density of zero were considered data voids and likely represent deep pool areas where the laser was unable to penetrate to the bottom. Areas with 4 or less points per 15 m2 were considered areas of low confidence due to a lack of surrounding data to confirm bathymetric elevations. It is likely that these are also deep areas. Areas with a point density of greater than 4 points per 15m2 were considered adequately covered with high confidence in the bathymetric data elevations represented. The confidence shapefile provided was created based on this information. By combining elevation data from the depth model and the point density data summarized within the confidence layer, overall depth penetration can be assessed (Figure 15,Table 10).

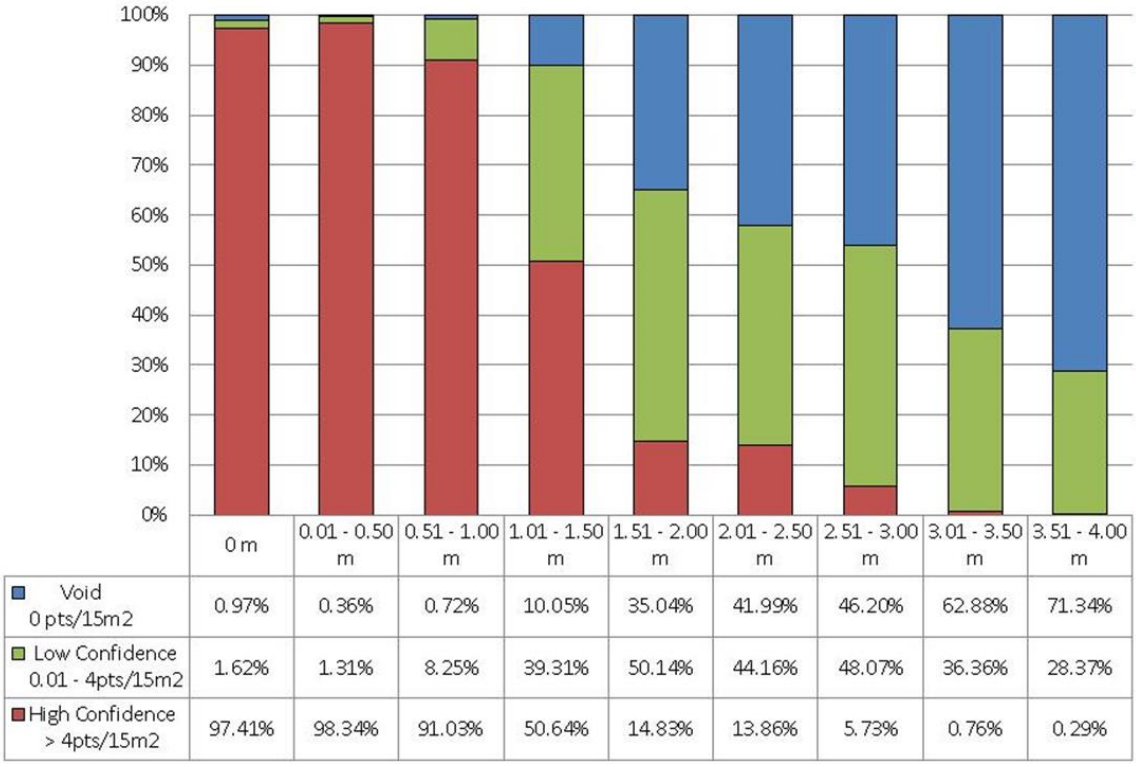

	0 m	0.01 - 0.50 m	0.51 - 1.00 m	1.01 - 1.50 m	1.51 - 2.00 m	2.01 - 2.50 m	2.51 - 3.00 m	3.01 - 3.50 m	3.51 - 4.00 m
Void 0 pts/15m2	0.97%	0.36%	0.72%	10.05%	35.04%	41.99%	46.20%	62.88%	71.34%
Low Confidence 0.01 - 4pts/15m2	1.62%	1.31%	8.25%	39.31%	50.14%	44.16%	48.07%	36.36%	28.37%
High Confidence > 4pts/15m2	97.41%	98.34%	91.03%	50.64%	14.83%	13.86%	5.73%	0.76%	0.29%

Figure 15: Confidence of depth penetration based on point density

Table 10: Bathymetric bottom return density

Cover classification	% of total area	Point Density
High Confidence	83%	1.96 points/m^2
Low Confidence	17%	0.11 points/m^2

It should be noted that confidence levels are designed for assessing the overall model of river topography at a spatial resolution of 1 square meter. In comparison to the channel cross section data, the interpolation of river bottom features is minimal.

Topo-Bathymetric LiDAR Accuracy

Channel cross sections surveyed by Atkins Geomatics were used to assess the accuracy of the LiDAR derived bottom topography. Because return density is an important factor influencing LiDAR accuracy results, separate statistics were calculated for the high and low confidence areas previously described (Table 10). The topo-bathymetric LiDAR demonstrated a vertical accuracy of 3-cm RMSE when compared to the 164 checkpoints taken on hard, bare earth surfaces. The bathymetric accuracy was assessed at 18.4 cm RMSE when compared to channel cross section measurements in the high confidence areas and 41.8 cm RMSE in the low confidence areas (Table 11).

The accuracy of the bathymetric data was assessed using the best ground survey data available; however, errors inherent to conventional cross section surveys are often difficult to quantify. These imprecisions are due to a number of factors but generally include local variability in the channel bottom, wading conditions, and GPS quality in heavily vegetation areas (see Appendix A, STARR 2013). By individually examining the classified LiDAR returns in relation to the surveyed cross sections, WSI observed two error conditions where the comparison between the ground survey and the LiDAR derived bathymetry created outliers.

The first condition was when the LiDAR returns within the water column were incorrectly classified as the channel bottom. Additionally, channel cross sections were found that appeared erroneous in relation to the topo-bathymetric surface. The invalid cross sections occurred in areas with heavy canopy suggesting that GPS quality was degraded. WSI screened the accuracy reports for outliers either caused by misclassified bathymetric bottom returns or invalid cross sections (Figure 16).

Table 11: Absolute and relative accuracies (meters) based on comparison to both hard surface check points and channel cross section points

	Bare Earth (Topo) Absolute Accuracy (Hard Surface RTK points)	High Confidence Bathymetric Accuracy (In Channel Points)	Low Confidence Bathymetric Accuracy (In Channel Points)
Sample	164	303	28
Average	<0.001	-0.051	-0.150
Median	0.004	-0.058	-0.248
RMSE	0.030	0.184	0.418
1σ	0.030	0.177	0.397
1.96σ	0.060	0.347	0.779

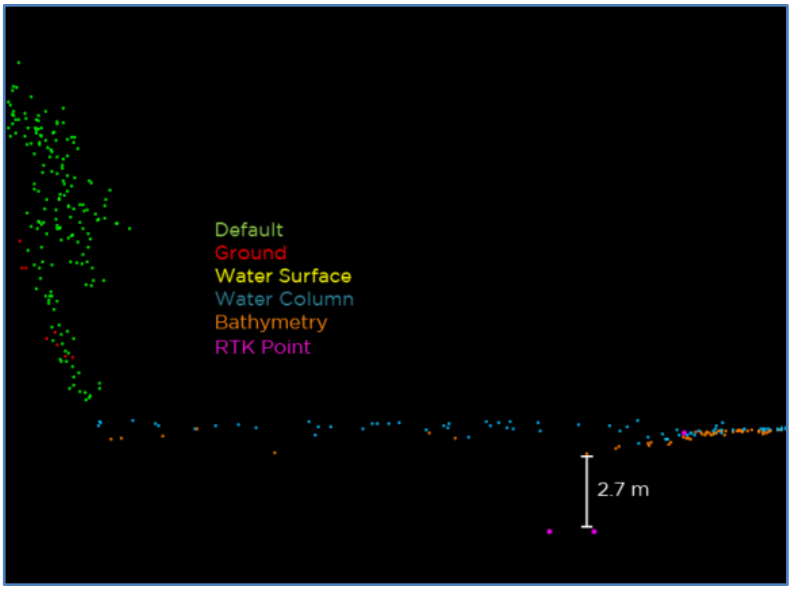

Figure 16: a) River channel cross section of steep bank dropoff where the bathymetric LiDAR returns in the water column were falsely classified as bathymetric bottom returns. These points were retained in the accuracy analysis

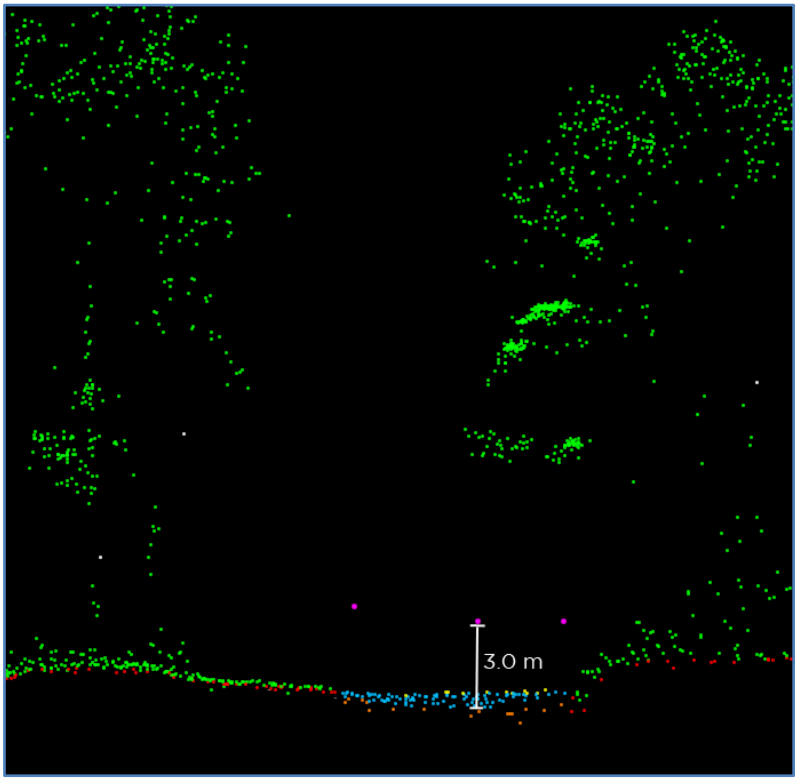

b) Cross section of a RTK transect under dense canopy where poor GPS signals have led to inaccurate measurements. These 3 points were removed from the accuracy analysis

Figure 17 and Figure 18 provide further comparisons of the topo-bathymetric LiDAR returns to the surveyed cross sections. The natural color digital imagery for each location are provided to illustrate water clarity, vegetation, and flow conditions at the transect location. These comparisons highlight the level of detail in the LiDAR derived bathymetry including small side channels and also show the ability of baythmetric LiDAR to map the channel in heavily vegetated areas where conventional GPS survey techniques are degraded or not possible (Figure 17 b and d). The images also illustrate the presence of outliers in both the surveyed channel cross sections and the classified LiDAR returns.

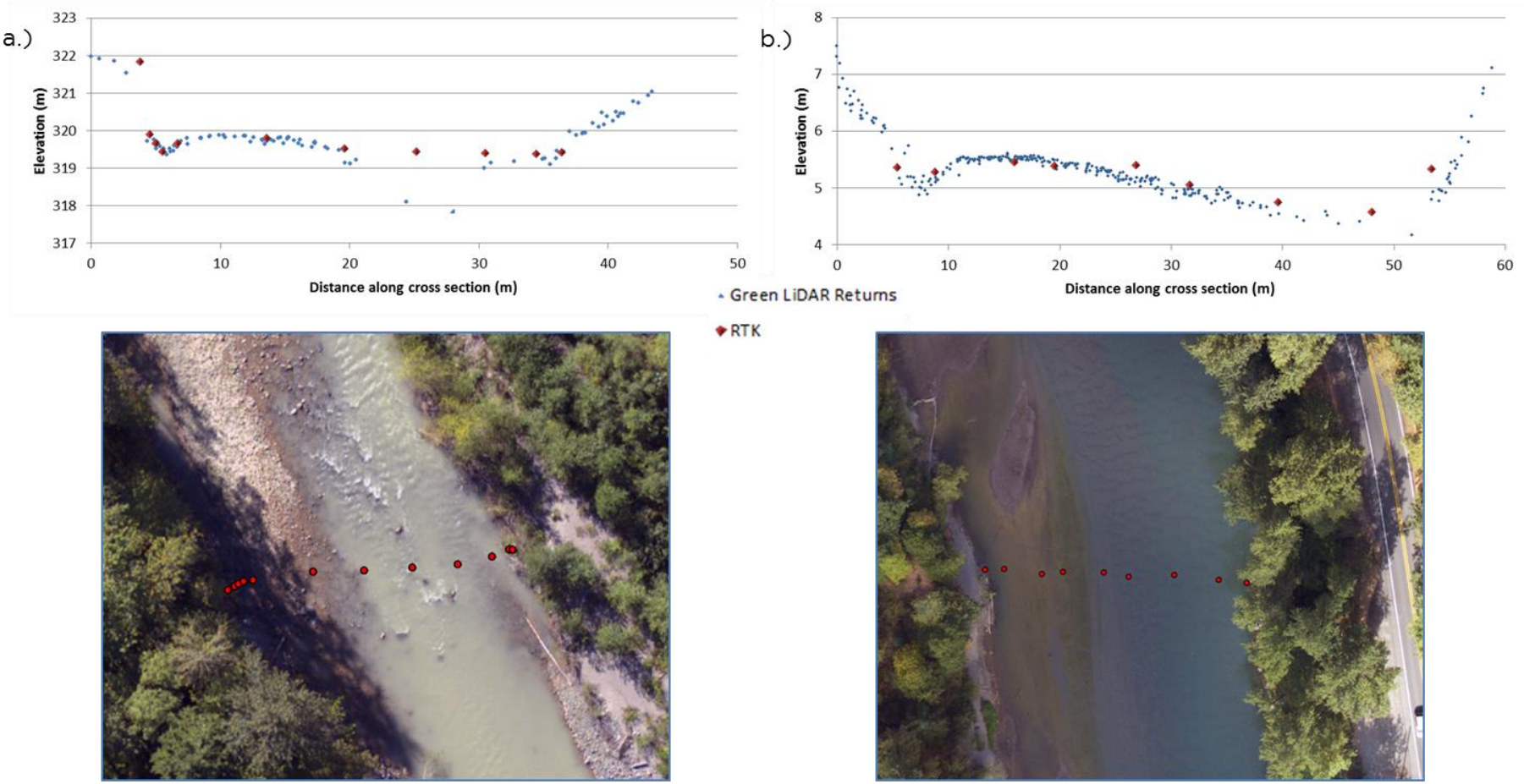

Figure 17: Example cross sections of topo-bathymetric LiDAR returns and channel cross section measurements with representative orthophotos. Note the x- and y-axis are not drawn to scale. (a) Demonstrates erroneous topo-bathymetric LiDAR returns due to channel depth, turbidity and water clarity. Beyond 1 Secchi depth (approx. 2.1 m) returns begin to lose accuracy. (b) Portrayal of a small side channel described by the green LiDAR, but not by the surveyed transect.

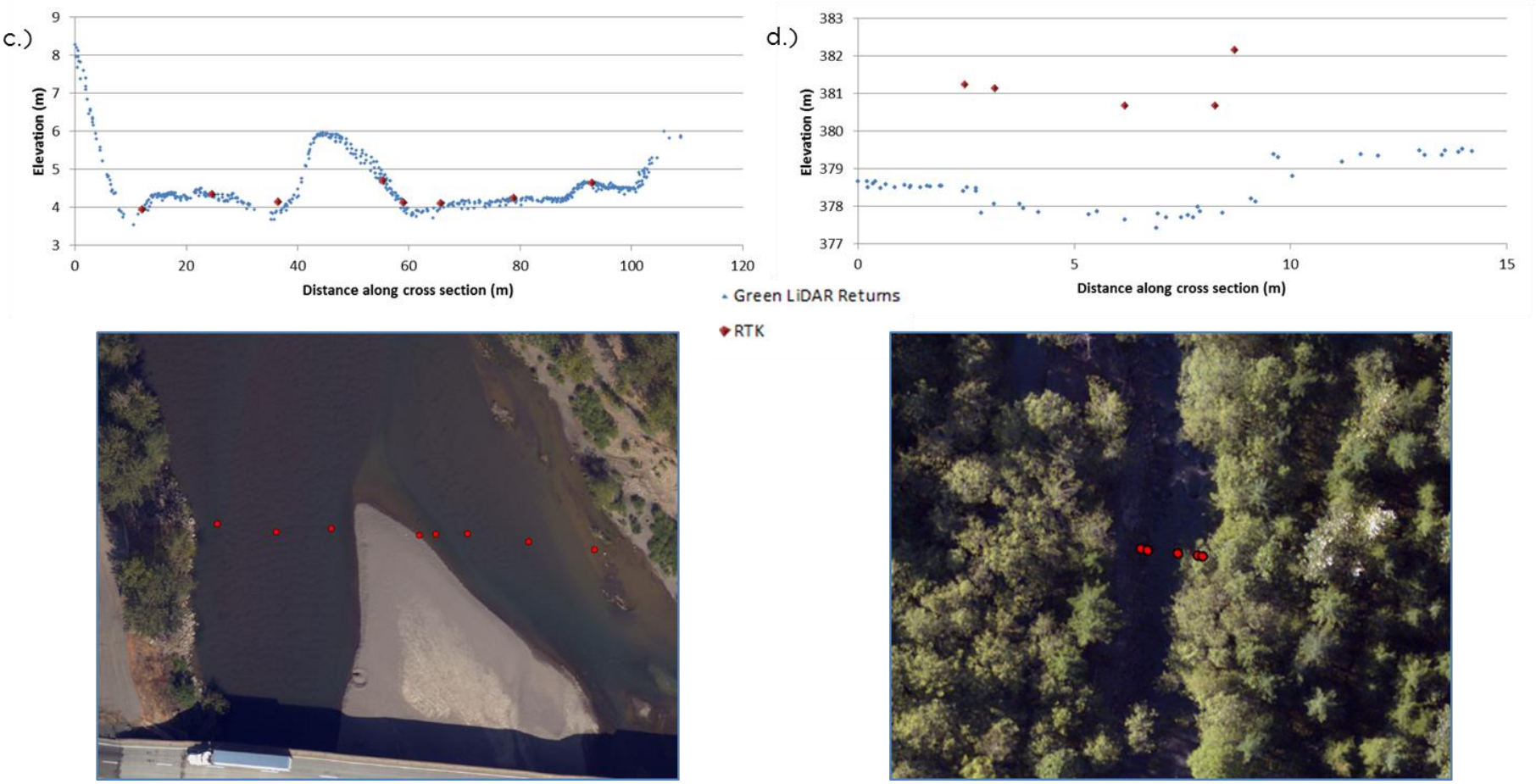

Figure 17 (cont.): (c) Shows tight agreement between RTK and green LiDAR returns generally found in less turbulent waters and depths within 1 Secchi depth. (d) Example of erroneous channel cross section measurements likely due poor GPS visibility.

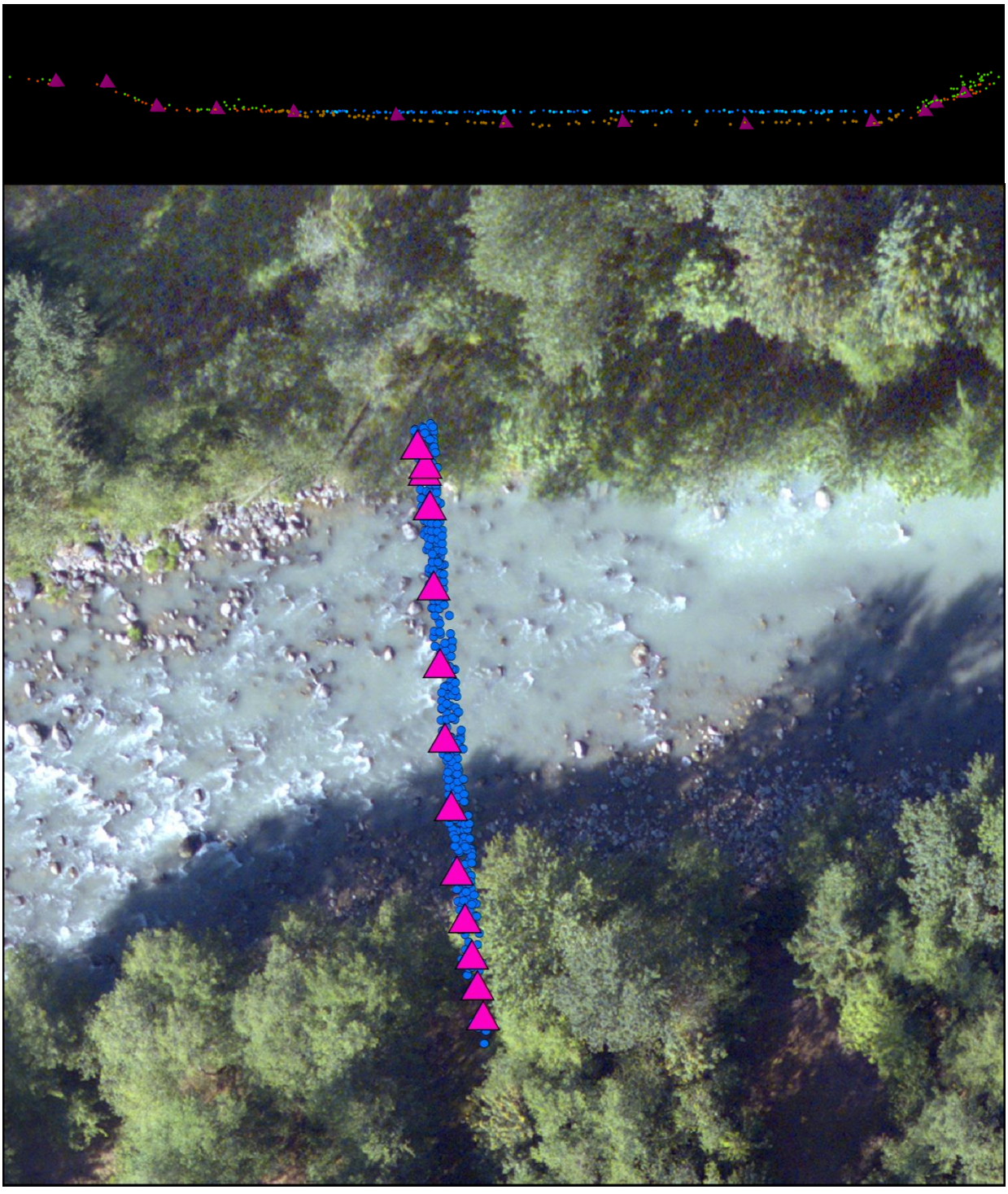

Figure 18: Sample bathymetric LiDAR cross-section. The blue points indicate the water surface, while the brown points indicate to the LiDAR derived bathymetric river bottom. Survey cross section measurements are shown as triangles.

Relative accuracy refers to the internal consistency of the data set as a whole: the ability to place an object in the same location given multiple flight lines, GPS conditions, and aircraft attitudes. When the LiDAR system is well calibrated, the swath-to-swath divergence is low (<0.10 meters). The relative accuracy is computed by comparing the ground surface model of each individual flight line with its neighbors in overlapping regions. The average line-to-line relative accuracy for the Sandy River LiDAR was 0.05 meters (Table 12, Figure 19).

Table 12: Relative accuracy of the Riegl VQ-820-G laser

	Relative Accuracy
Sample	63 surfaces
Average	0.047
Median	0.048
RMSE	0.049
1σ	0.008
1.96σ	0.015

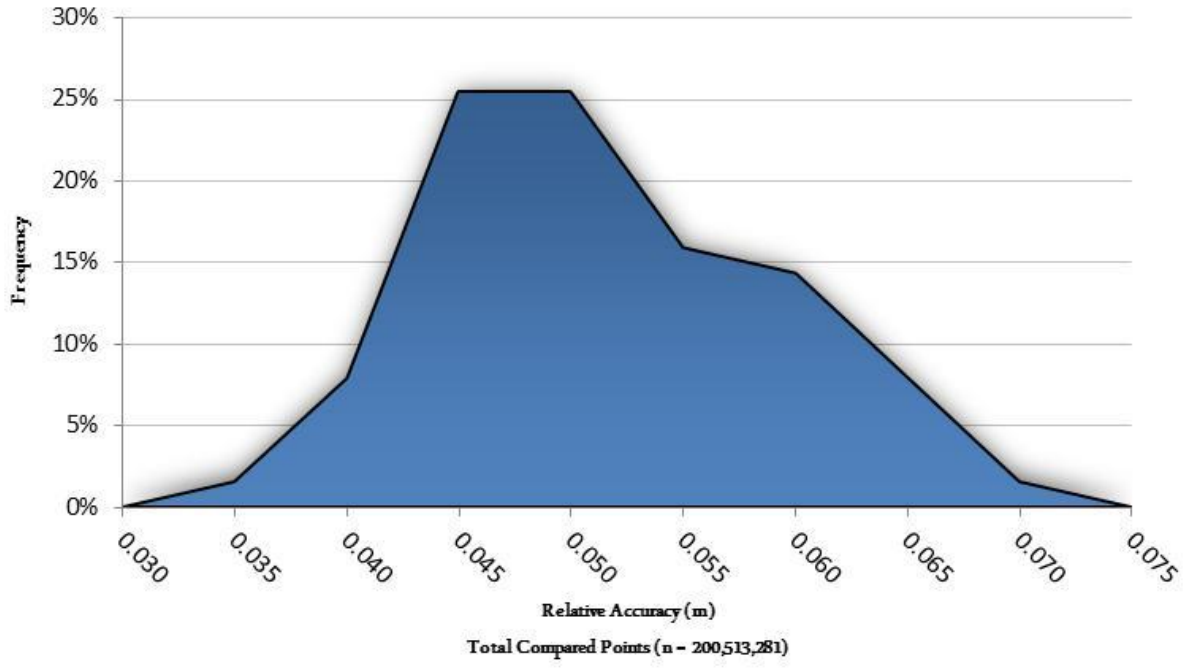

Figure 19: Frequency plot for relative accuracy between flight lines of the Riegl VQ-820-G laser

DISCUSSION

The goal of this project was to test and quantify the effectiveness of cutting edge small footprint, topo-bathymetric LiDAR technology in a Pacific Northwest riverine environment. The Sandy River, Oregon was of particular interest because of the removal of the Marmot Dam in 2007 and the subsequent monitoring of downstream sediment transport and geomorphic response. In the fall of 2012, WSI mapped ~43 miles of the Sandy River from its mouth upstream to the confluence of the Zig Zag River using the Riegl VQ-820-G airborne hydrographic airborne laser scanner.

Water depths ≤ 1.5 meters were mapped with high confidence. As might be expected, the confidence progressively decreased with increasing water depth, but some level of confidence was retained for over 50% of the mapped area (between 2.5-3.0 meters). The analysis indicated that 83% of the river was mapped with high confidence and depth penetration was consistent with the system specification of 1-Secchi depth. A confidence layer is provided with the deliverables and should be used to help delineate areas where bottom return data is suspect (a good indicator of increased water depth).

WSI defined high/low confidence based on bottom returns within a 15 m^2 area centered on any given 1 m^2 cell. This definition was based on visual inspection of the data (especially in known deep pools) and assumes that a lack of bottom return density is indicative of depths exceeding the capability of the instrument in this setting. A potential source of error does inherently lie within the dataset. In areas where the depth exceeds the ability of the laser to detect the bottom, water column points within the penetrable depths of the water are collected. Due to the nature of the grounding algorithm used to classify the bathymetry points, the lowest perceivable water column points can be improperly identified as bathymetry. This can lead to improper density reporting and false confidence in depth measurements. This indicates the need for further sophistication of confidence models and ultimately better characterization of bathymetric returns.

The accuracy of the topo-bathymetric elevations for terrestrial surfaces was 3-cm (RMSE) when compared to check points on hard bare earth surfaces. These results were consistent with values WSI achieves with its NIR topographic LiDAR systems. The accuracy of the bathymetric (or channel bottom) returns was 18.4 cm for high confidence areas as assessed against surveyed channel cross section points. As noted in the results, the accuracy of the channel cross section survey was more difficult to assess than the terrestrial based survey. Sub-surface variability combined with difficult wading conditions can introduce errors into the channel cross section measurements. In addition, GPS may be degraded in a heavily vegetated river canyon resulting in elevation measurement errors. Given the uncertainty (and temporal differences) in the transect data, we felt that the measured bathymetric accuracy was well within expectations and validated refraction corrections.

The project included the co-acquisition of topo-bathymetric (green) LiDAR, NIR topographic LiDAR, and natural color digital imagery. We found that the topo-bathymetric LiDAR did not record a surface and bottom return for certain water surface conditions. This was particularly true in very shallow water areas where surface/bottom returns are convolved or non-existent in the waveform. Consequently, we found that the NIR LiDAR data was essential to creating a 3-D water-mask to help to define the water surface which greatly facilitated the refraction computation of the bathymetric LiDAR returns.

Moving forward, we are investigating more advanced processing techniques to eliminate false classification of bottom returns in deep water due to returns from within the water column. These methods include a more sophisticated utilization of the full waveform data along with evaluation of local density statistics and grounding algorithms. The misclassification of bottom returns is considered a deficiency in processing methods rather than a limitation of technology. The development of these techniques is considered a priority due to the potential implications of these types of errors in applications such as hydraulic flow modeling.

Overall, the project produced encouraging results for the utilization of small footprint, topo-bathymetric LiDAR for mapping channel floodplains and shallow water bathymetry. As stated by McKean et. al. (2009), "the capability to map, with relatively high resolution, large portions of channel networks challenges us to think beyond conventional channel cross sections and maps of short reaches of streams, and instead describe and investigate spatial patterns and connectivity of riverine and riparian habitat, aquatic processes and the interactions with channel biota at up to watershed scales."[3] While we could not map the deepest pools in the Sandy, we were able to confidently map 83% of the wetted channel including side channel and off-channel areas that are notoriously difficult to measure using conventional techniques. The topo-bathymetric LiDAR provides subsurface detail at a higher level of detail than the traditional cross section approach provides and maps areas that would otherwise be unfeasible or inefficient for water-borne SONAR surveys.

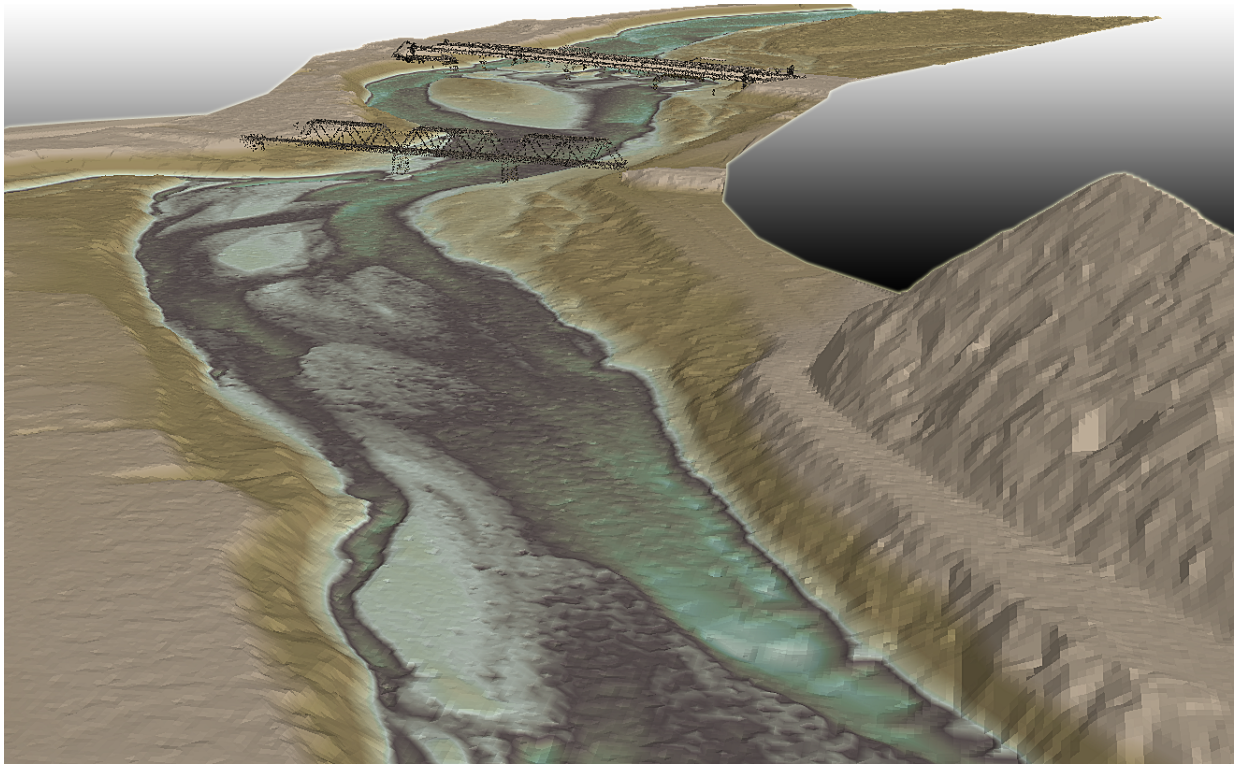

[3] McKean, J., D. Nagel, D. Tonina, P. Bailey, C.W. Wright, C. Bohn, and A. Nayegandhi. 2009. Remote Sensing of Channels and Riparian Zones with a Narrow-Beam Aquatic-Terrestrial LiDAR. *Remote Sensing*; 1(4):1065-196.

The section below summarizes the NIR LiDAR and natural color digital imagery that was acquired to provide a secondary data set to compare and complement the topo-bathymetric collection. Data specifications, processing, and statistical results are provided. For NIR LiDAR acquisition specifications, refer to the Airborne Survey section above.

NIR LiDAR Data Processing

For the NIR LiDAR, WSI processing staff initiated a suite of automated and manual techniques to process the data into the requested deliverables. Processing tasks include GPS control computations, kinematic corrections, calculation of laser point position, calibration for optimal relative and absolute accuracy, and classification of ground and non-ground points (Table 13, Figure 20). Processing methodologies are tailored for the landscape and intended application of the point data. A full description of these tasks can be found in Table 14.

Table 13: ASPRS LAS classification standards applied to NIR LiDAR dataset

Classification Number	Classification Name	Classification Description
1	Default/ Unclassified	Laser returns that are not included in the ground class and not dismissed as Noise.
2	Ground	Ground that is determined by a number of automated and manual cleaning algorithms to determine the best ground model the data can support.

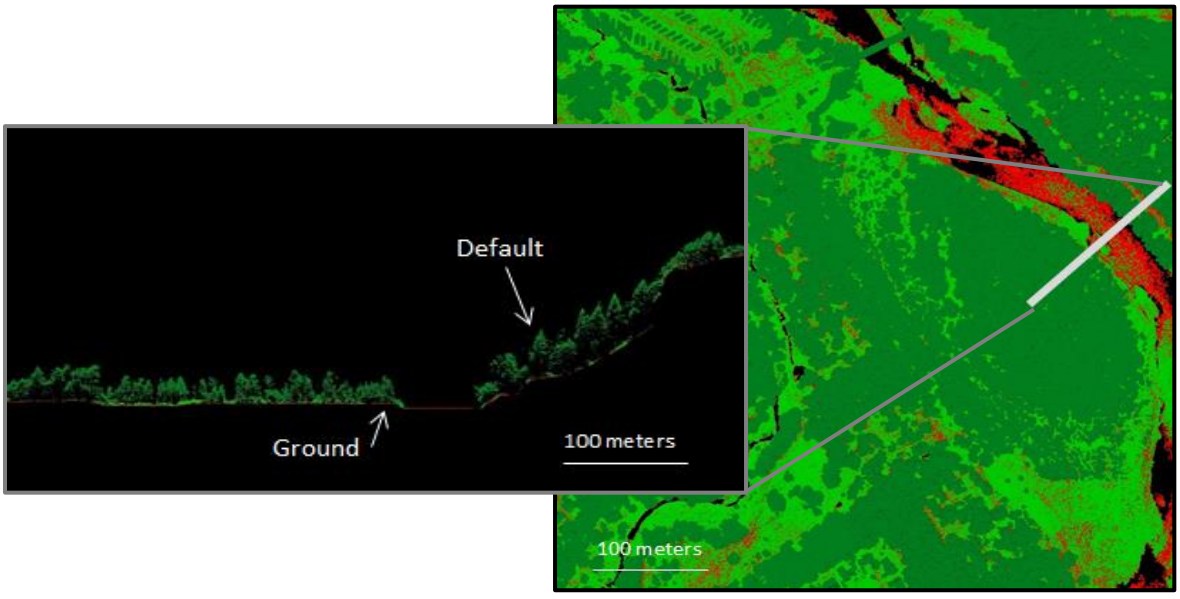

Figure 20: Cross section demonstrating classification scheme used for the NIR LiDAR data

Table 14: NIR LiDAR processing workflow

LiDAR Processing Step	Software Used
Resolve kinematic corrections for aircraft position data using kinematic aircraft GPS and static ground GPS data.	Waypoint GPS v.8.3 Trimble Business Center v.2.80 Blue Marble Desktop v.2.5
Develop a smoothed best estimate of trajectory (SBET) file that blends post-processed aircraft position with attitude data. Sensor head position and attitude are calculated throughout the survey. The SBET data are used extensively for laser point processing.	IPAS TC v.3.1
Calculate laser point position by associating SBET position to each laser point return time, scan angle, intensity, etc. Create raw laser point cloud data for the entire survey in *.las (ASPRS v. 1.2) format. Data are converted to orthometric elevations (NAVD88) by applying a Geoid12 correction.	ALS Post Processing Software v.2.74
Import raw laser points into manageable blocks (less than 500 MB) to perform manual relative accuracy calibration and filter erroneous points. Ground points are then classified for individual flight lines (to be used for relative accuracy testing and calibration).	TerraScan v.12.004
Test relative accuracy sing ground classified points per each flight line. Automated line-to-line calibrations are then performed for system attitude parameters (pitch, roll, heading), mirror flex (scale) and GPS/IMU drift. Calibrations are calculated on ground classified points from paired flight lines and results are applied to all points in a flight line. Every flight line is used for relative accuracy calibration.	TerraMatch v.12.001
Classify resulting data to ground and other client designated ASPRS classifications (Table 13). Assess statistical absolute accuracy via direct comparisons of ground classified points to ground RTK survey data.	TerraScan v.12.004 TerraModeler v.12.002
Generate bare earth models as triangulated surfaces. Highest hit models were created as a surface expression of all classified points (excluding the noise and withheld classes). All surface models were exported as ESRI grids at a 1 meter pixel resolution.	TerraScan v.12.004 ArcMap v. 10.1 TerraModeler v.12.002

NIR LiDAR Results

Density Results

The average first-return density for the NIR LiDAR data for the Sandy River project area was 9.57 points/m^2 (Table 15). The pulse density distribution will vary within the study area due to laser scan pattern and flight condition. Some types of surfaces (i.e. breaks in terrain, dense vegetation, water, steep slopes) may return fewer pulses to the sensor (delivered density) than originally emitted by the laser (native density).

The statistical distribution of first returns (Figure 21) and classified ground points (Figure 22) are portrayed below. Also presented are the spatial distribution of average first return densities (Figure 23) and ground point densities (**Error! Reference source not found.**) for each 100-m^2 cell.

Table 15: Average LiDAR point densities

Classification	Point Density
First-Return	9.57 points/m^2
Ground Classified	1.52 points/m^2

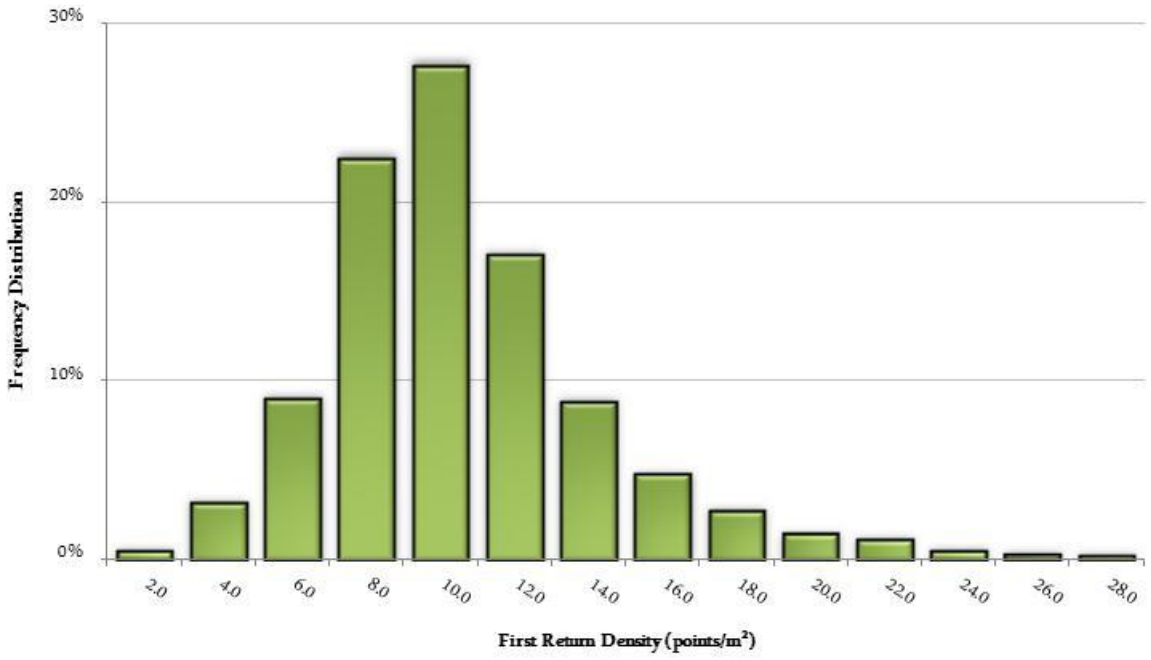

Figure 21: Frequency distribution of first return (native) densities of the 100m2 gridded sample area

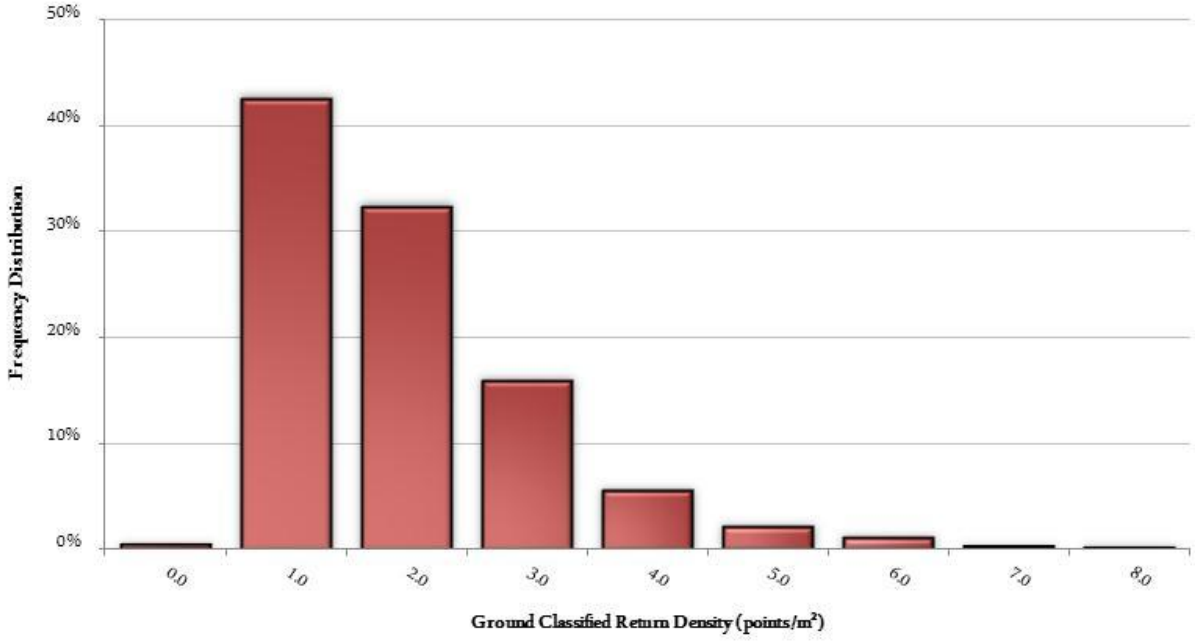

Figure 22: Frequency distribution of ground classified returns of the 100m^2 gridded sample area

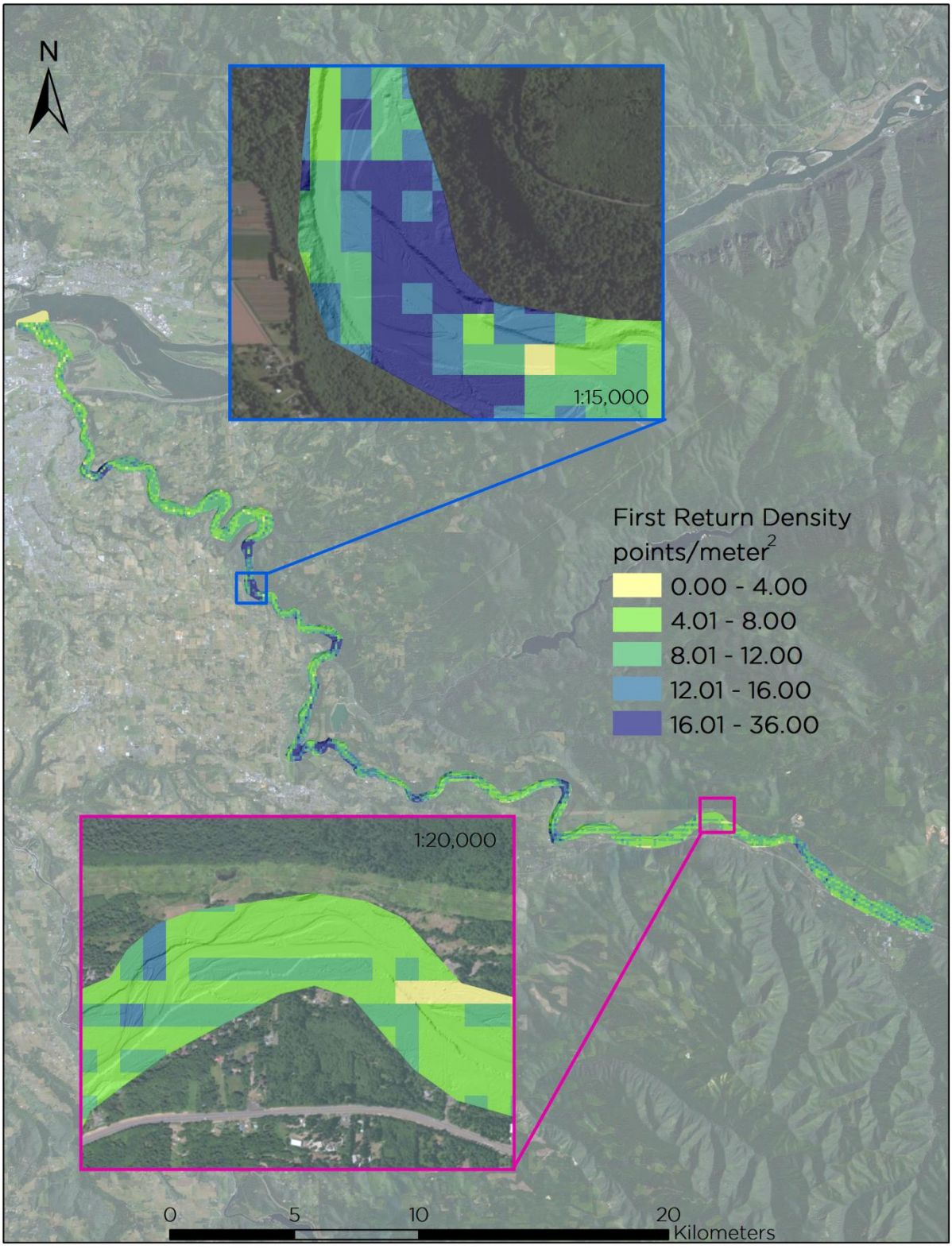

Figure 23: Native density map for the Sandy River LiDAR site

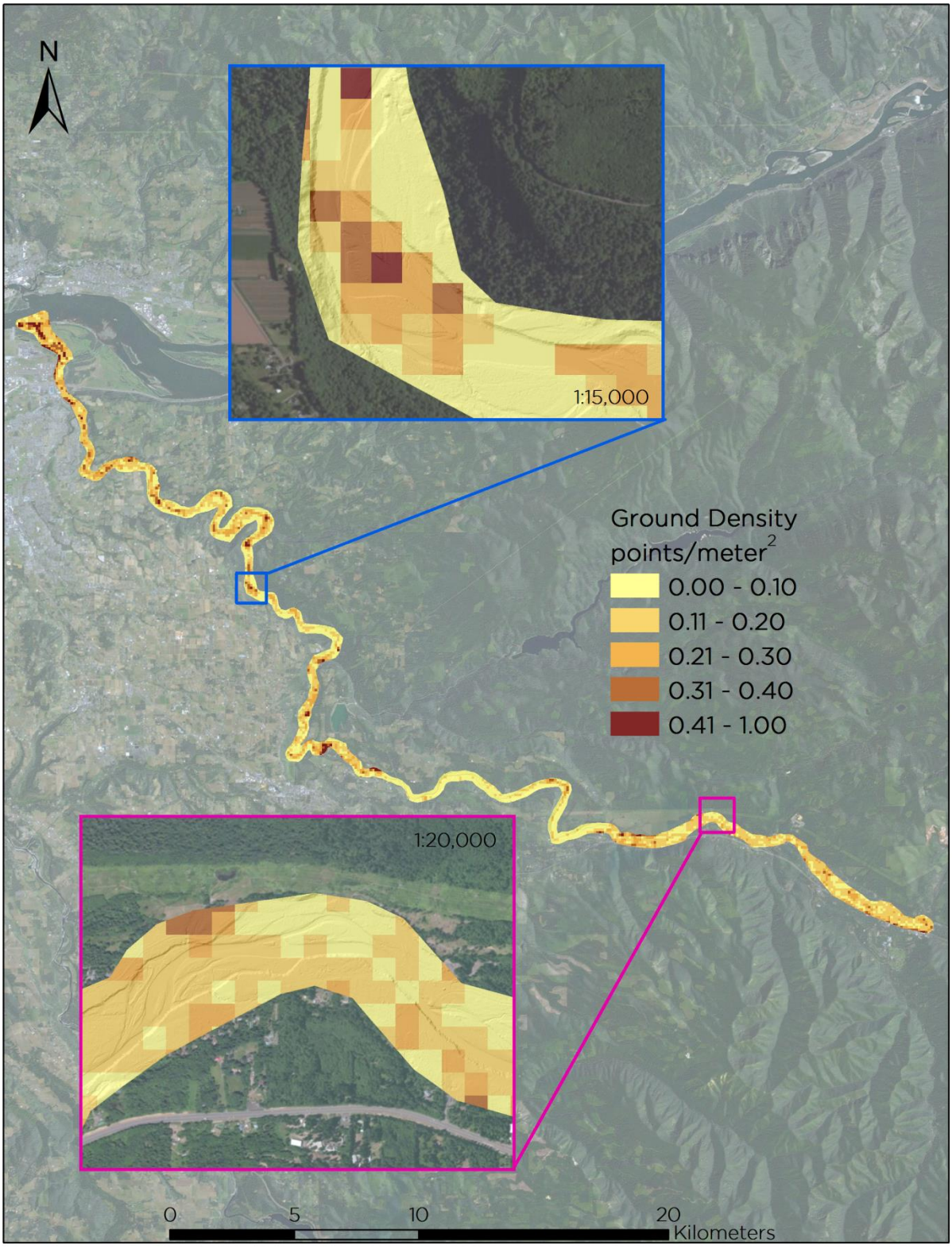

Figure 24: Ground density map for the Sandy River LiDAR site

NIR LiDAR Accuracy

The accuracy of the LiDAR data collection can be described in terms of absolute accuracy (the consistency of the data with external data sources) and relative accuracy (the consistency of the dataset with itself). See Appendix A and B for further information on sources of error and operational measures used to improve relative accuracy.

LiDAR Absolute Accuracy

Vertical absolute accuracy was primarily assessed from RTK ground check point (GCP) data collected on open, bare earth surfaces with level slope (<20°). Fundamental Vertical Accuracy (FVA) reporting is designed to meet guidelines presented in the National Standard for Spatial Data Accuracy (FGDC, 1998). FVA compares known RTK ground survey check points to the triangulated ground surface generated by the LiDAR points. FVA is a measure of the accuracy of LiDAR point data in open areas where the LiDAR system has a "very high probability" of measuring the ground surface and is evaluated at the 95% confidence interval (1.96 σ).

Absolute accuracy is described as the mean and standard deviation (sigma σ) of divergence of the ground surface model from ground survey point coordinates. These statistics assume the error for x, y, and z is normally distributed, and therefore the skew and kurtosis of distributions are also considered when evaluating error statistics. For the Sandy River LiDAR survey, 164 RTK points were collected in total resulting in an average accuracy of -0.007 meters (Table 16, Figure 25).

Table 16: Absolute and relative accuracies

	Absolute Accuracy	Relative Accuracy
Sample	164 points	68 surfaces
Average	-0.007 m	0.026 m
Median	-0.009 m	0.028 m
RMSE	0.020 m	0.031 m
1σ	0.019 m	0.008 m
2σ	0.037 m	0.015 m

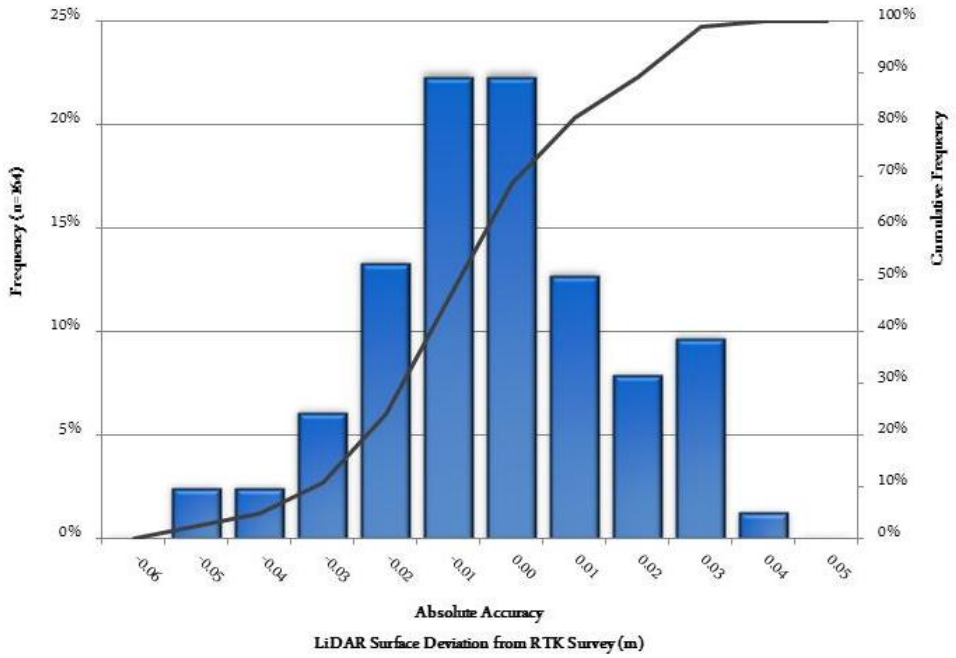

Figure 25: Frequency histogram for LiDAR surface deviation from RTK values

LiDAR Relative Accuracy

Relative accuracy refers to the internal consistency of the data set as a whole: the ability to place an object in the same location given multiple flight lines, GPS conditions, and aircraft attitudes. When the LiDAR system is well calibrated, the swath-to-swath divergence is low (<0.10 meters). The relative accuracy is computed by comparing the ground surface model of each individual flight line with its neighbors in overlapping regions. The average relative accuracy for the Sandy River LiDAR was 0.026 meters (Table 16, Figure 26).

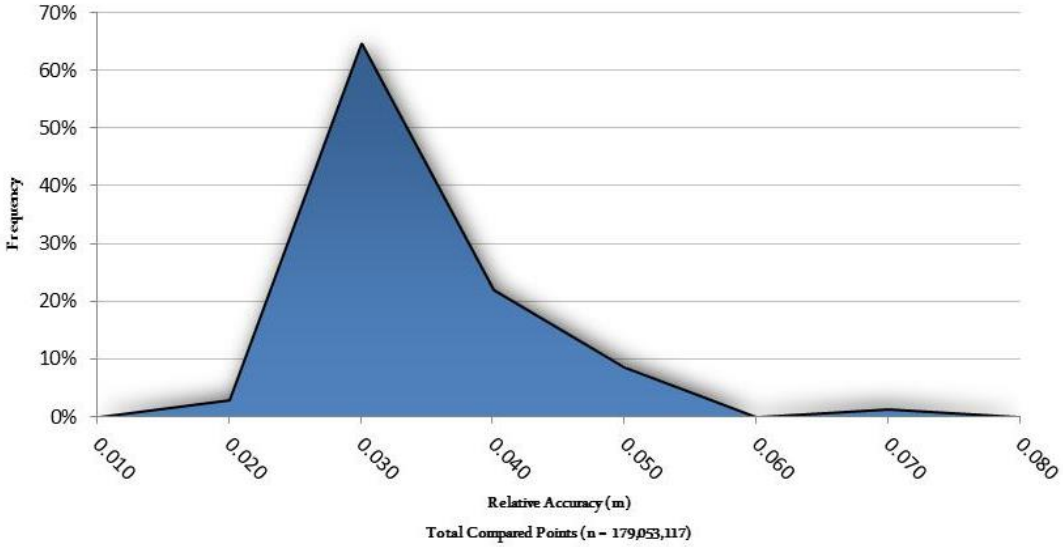

Figure 26: Frequency plot for relative accuracy between flight lines

Digital Imagery Acquisition

The aerial imagery was acquired with the NIR and topobathymetric LiDAR using a Leica RCD105 39-megapixel digital camera. Images were collected in 3 spectral bands (red, green, and blue) with 60% along track overlap and 30% side-lap between frames. The acquisition flight parameters were designed to yield a native pixel resolution of 7.0 centimeters. The resulting spatial accuracies (RMSE) were routinely ≤ 21.0 centimeters at 95% confidence level. Orthophoto specifications particular to the Sandy River digital imagery are shown in Table 17.

Table 17: Project-specific orthophoto specifications

Sandy River Orthophotography Specifications	
Focal Length	60 mm
Data Format	RGB
Camera Pixel Size	6.8 µm
Image Size	7,216 x 5,412 pixels
Frame Rate	2.2 seconds
FOV	45°
Equipment	RCD 105
Spectral Bands	Red, Green, Blue
Ground Resolution	7-cm pixel size
Along Track Overlap	≥60%
Planned Height (AGL)	600 meters
GPS Baselines	≤13 nm
GPS PDOP	≤3.0
GPS Satellite Constellation	≥6
Horizontal Accuracy	21 centimeters
Image	8-bit GeoTiff

Digital Imagery Processing

The collected digital photographs went through multiple processing steps to create final orthophoto products. Image radiometric values were calibrated to specific gain and exposure settings, and photo position and orientation were calculated by linking the time of image capture to the smoothed best estimate of trajectory (SBET). Within Leica Photogrammetry Suite (LPS), the exterior orientation derived from the SBET was applied to the photo images and the interior orientation of the camera was defined. Adjusted images were orthorectified using the LiDAR-derived ground model to remove displacement effects from topographic relief inherent in the imagery and individual orthorectified TIFFs were blended together to remove seams. The final mosaics were corrected for any remaining radiometric differences between images using Inpho's OrthoVista. The processing workflow for orthophotos is summarized in Table 18.

Table 18: Orthophoto processing workflow

Orthophoto Processing Step	Software Used
Resolve GPS kinematic corrections for the aircraft position data using kinematic aircraft GPS (collected at 2HS) and static ground GPS (1Hz) data collected over geodetic controls.	IPAS TC v. 3.1
Develop a smooth best estimate trajectory (SBET) file that blends post-processed aircraft position with attitude data. Sensor heading, position, and attitude are calculated throughout the survey.	IPAS TC v. 3.1
Create an exterior orientation file (EO) for each photo image with omega, phi, and kappa.	IPAS CO v 1.3
Develop raw photos into 8-bit tiffs, applying necessary radiometric corrections.	Leica Calibration Post Processor 1.1.2
Apply EO to photos, measure ground control points and perform aerial triangulation.	Leica Photogrammetry Suite 2011
Import DEM, orthorectify and clip triangulated photos to the specified area of interest.	Leica Photogrammetry Suite 2011
Mosaic orthorectified imagery, blending seams between individual photos and correcting for radiometric differences between photos.	Inpho v. 5.5

Digital Imagery Accuracy

Image accuracy is measured by independent ground check points (GCPs) identified on the LiDAR intensity images in areas of clear visibility. Once the ground check points were identified in the NIR LiDAR intensity images, the exact spot was identified in the orthophotography and the displacement was recorded for further statistical analysis (Figure 27). **Error! Reference source not found.**shows the distribution of GCPs used to assess the accuracy of the digital imagery.

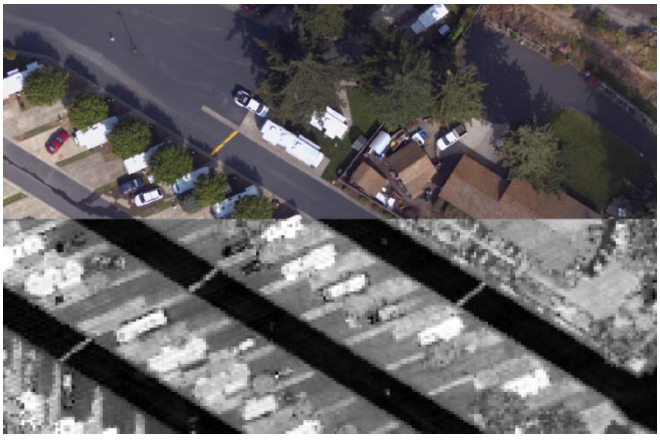

Figure 27: Image displaying the co-registration between the LiDAR intensity image and the orthophoto at a location within the Sandy River LiDAR site

Figure 28: Location of GCPS used to assess the accuracy of the Sandy River orthoimagery

The cumulative orthophoto horizontal accuracy for the Sandy River LiDAR site was 0.13 meters measured by ground control points, meeting our accuracy standard of <3 pixels (< 0.21 meters) (Table 19). Figure 29 contains a scatterplot showing congruence between LiDAR intensity images and orthophotos in aerial target locations.

Table 19: Orthophotography accuracy statistics for Sandy River LiDAR

Sandy River LiDAR Photo Accuracy	
Mean	0.13 m
RMSE	0.29 m
1σ	0.25 m
1.96 σ	0.50 m

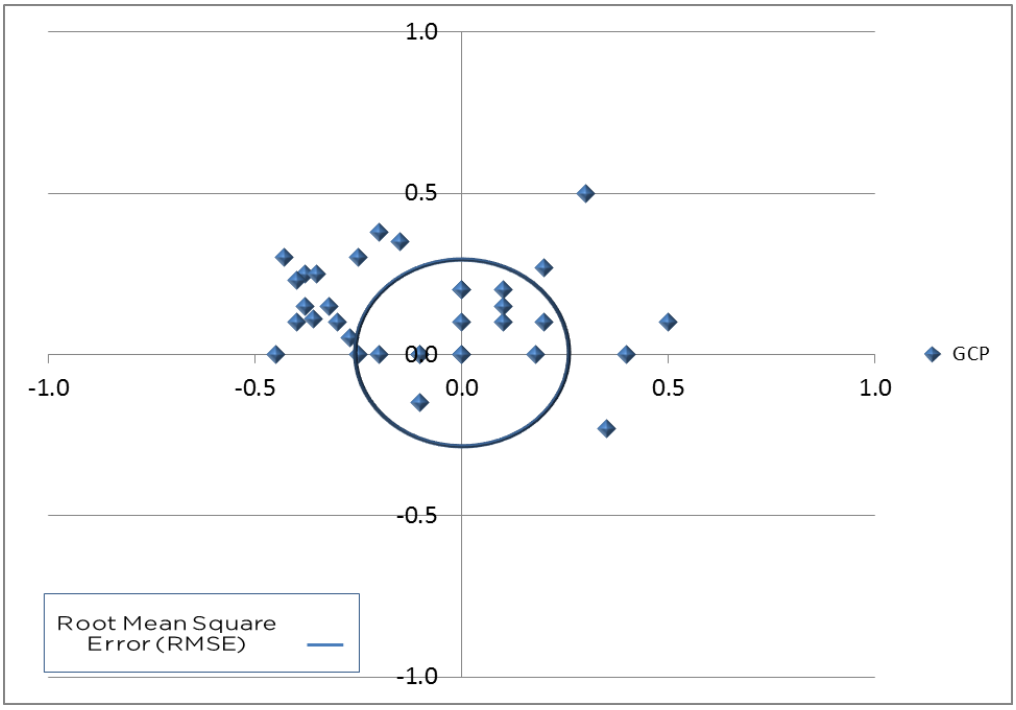

Figure 29: Scatterplot displaying the XY deviation of GCPs between the orthophoto imagery and the LiDAR intensity images

CERTIFICATIONS

WSI provided LiDAR services for the Sandy River Data study area as described in this report.

I, Russ Faux, have reviewed the attached report for completeness and hereby state that it is a complete and accurate report of this project.

_____

Russ Faux
Principal
WSI

I, Christopher W. Yotter-Brown, being first dully sworn, say that as described in the Ground Survey subsection of the Acquisition section of this report was completed by me or under my direct supervision and was completed using commonly accepted standard practices. Accuracy statistics shown in the Accuracy Section have been reviewed by me to meet National Standard for Spatial Data Accuracy.

Christopher W. Yotter-Brown, PLS Oregon & Washington
WSI
Portland, OR 97204

REGISTERED PROFESSIONAL LAND SURVEYOR
OREGON
JULY 13, 2004
Christopher W. Yotter - Brown
60499 LS

3/19/2013

RENEWAL DATE: 6/30/2014

Figure 30: Comparison of green and NIR LiDAR bare-earth models. The top image was created from green LiDAR ground and bottom bathymetric returns showing full channel expression. The bottom image was created from the NIR LiDAR ground returns demonstrating heavy TIN-ing across the stream channel. The outline in red represents the water's edge breakline.

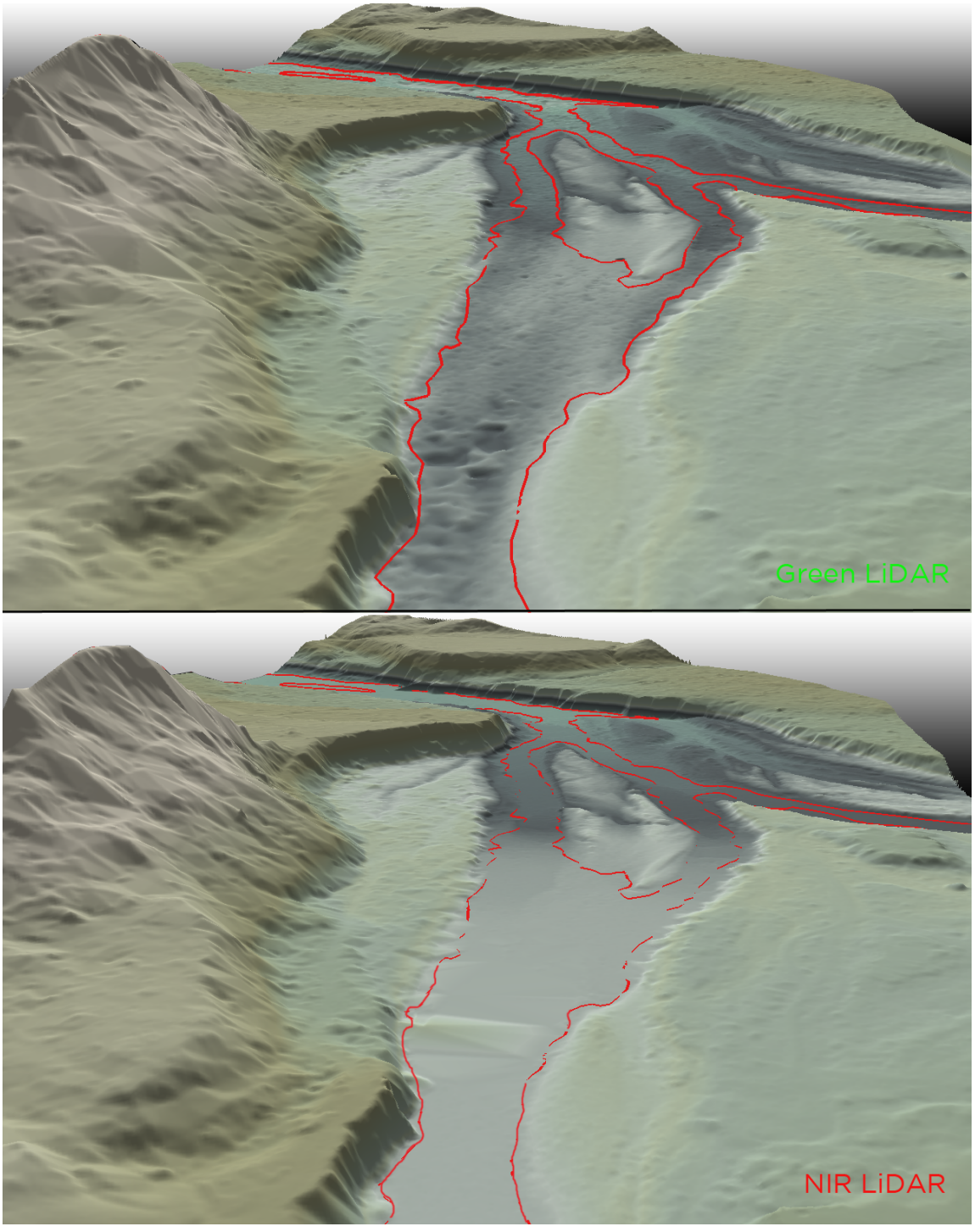

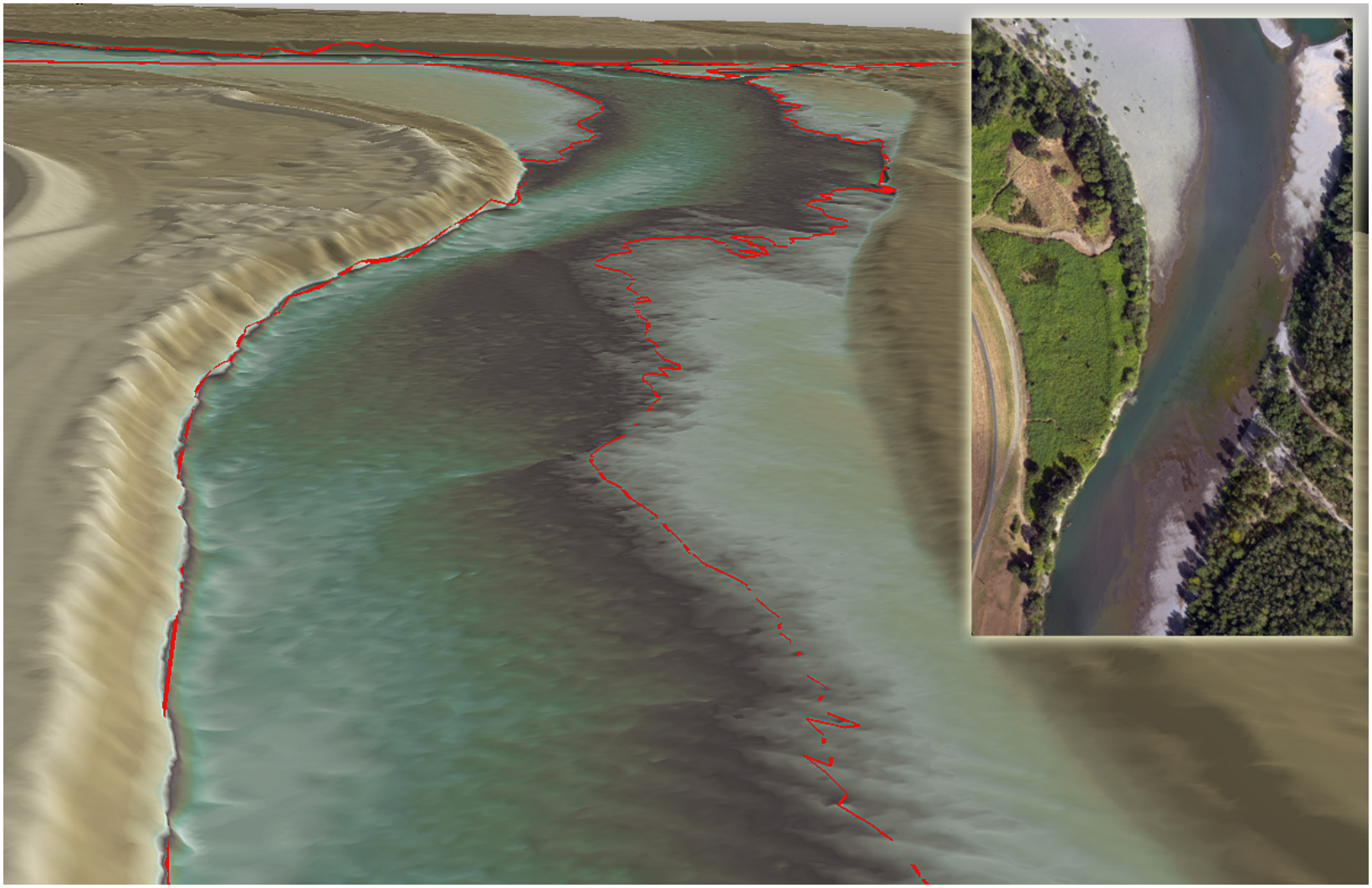

Figure 31: Bathymetric model colored by elevation just east of the Sandy Water Treatment Plant; the red outline is the water breakline. The right corner panel shows the orthophotos representing the highlighted stretch of the Sandy River.

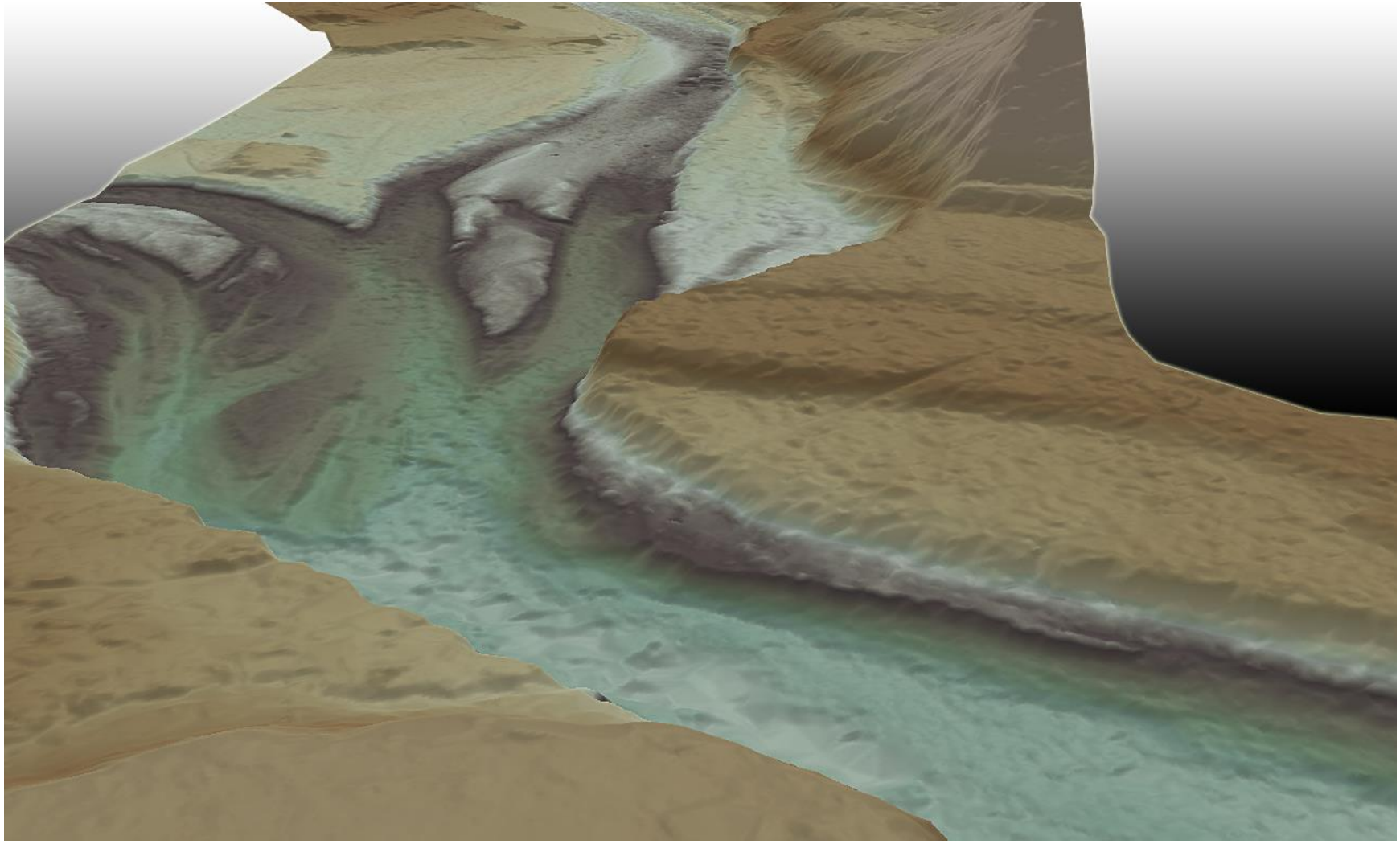

Figure 32: Bathymetric gridded model of ground and bathymetric bottom LiDAR returns colored by elevation. The scene is looking west at the junction of the Snake and Bull Run River.

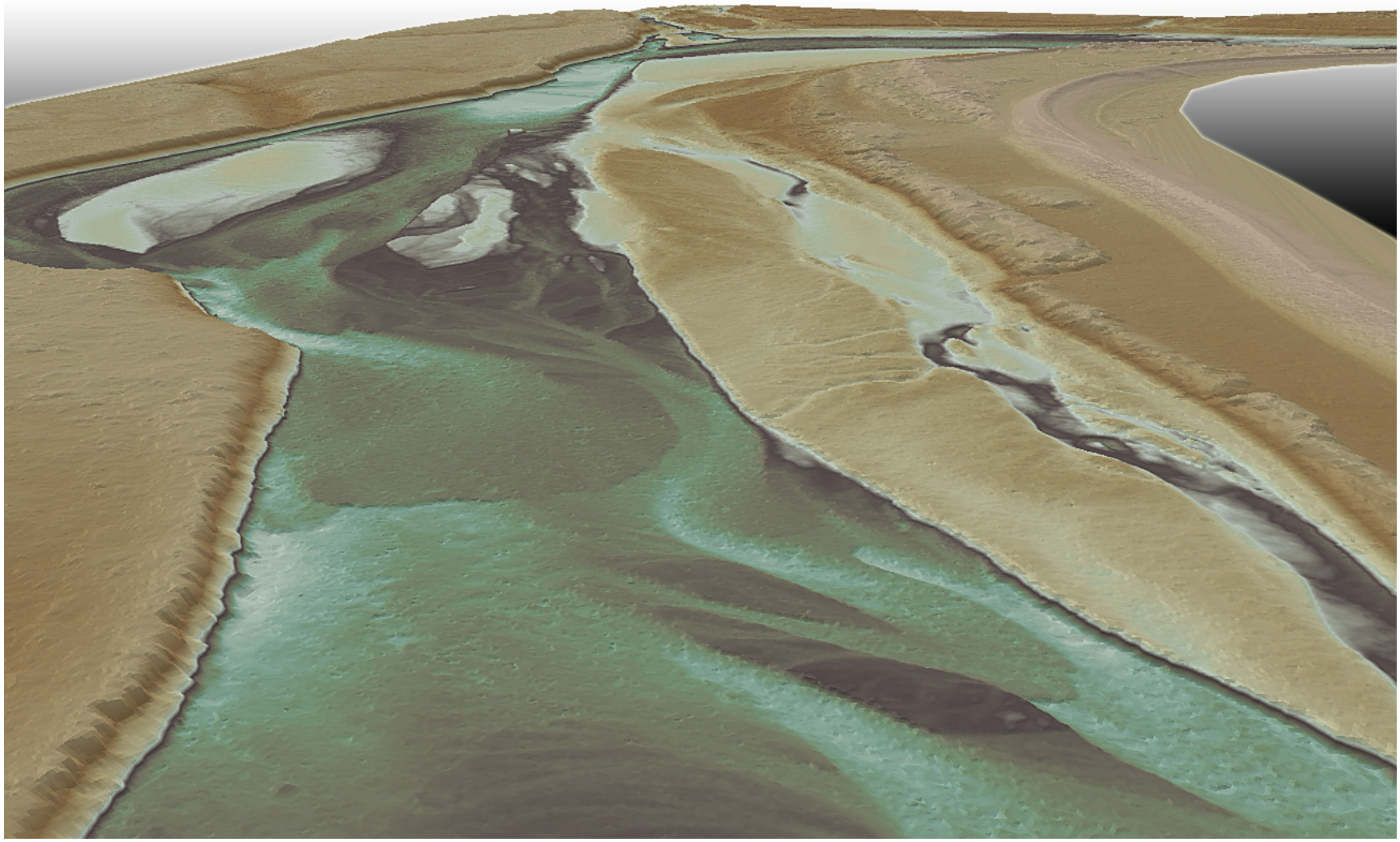

Figure 33: Bathymetric model of ground and bathymetric bottom classified LiDAR returns colored by elevation. The scene is looking east along the Sandy River Park reach of the Sandy River.

GLOSSARY

1-sigma (σ) Absolute Deviation: Value for which the data are within one standard deviation (approximately 68th percentile) of a normally distributed data set.

1.96-sigma (σ) Absolute Deviation: Value for which the data are within two standard deviations (approximately 95th percentile) of a normally distributed data set.

Root Mean Square Error (RMSE): A statistic used to approximate the difference between real-world points and the LiDAR points. It is calculated by squaring all the values, then taking the average of the squares and taking the square root of the average.

Secchi Depth: An estimate of water clarity measured by lowering a disk into water and recording the depth at which it disappears from sight. This measured depth at which light no longer penetrates the water column is known as the Secchi Depth.

Pulse Rate (PR): The rate at which laser pulses are emitted from the sensor; typically measured as thousands of pulses per second (kHz).

Pulse Returns: For every laser pulse emitted, the Leica ALS 60 system can record *up to four* wave forms reflected back to the sensor. Portions of the wave form that return earliest are the highest element in multi-tiered surfaces such as vegetation. Portions of the wave form that return last are the lowest element in multi-tiered surfaces.

Accuracy: The statistical comparison between known (surveyed) points and laser points. Typically measured as the standard deviation (sigma σ) and root mean square error (RMSE).

Intensity Values: The peak power ratio of the laser return to the emitted laser. It is a function of surface reflectivity.

Data Density: A common measure of LiDAR resolution, measured as points per square meter.

Spot Spacing: Also a measure of LiDAR resolution, measured as the average distance between laser points.

Nadir: A single point or locus of points on the surface of the earth directly below a sensor as it progresses along its flight line.

Scan Angle: The angle from nadir to the edge of the scan, measured in degrees. Laser point accuracy typically decreases as scan angles increase.

Overlap: The area shared between flight lines, typically measured in percent; 100% overlap is essential to ensure complete coverage and reduce laser shadows.

DTM / DEM: These often-interchanged terms refer to models made from laser points. The digital elevation model (DEM) refers to all surfaces, including bare ground and vegetation, while the digital terrain model (DTM) refers only to those points classified as ground.

Real-Time Kinematic (RTK) Survey: GPS surveying is conducted with a GPS base station deployed over a known monument with a radio connection to a GPS rover. Both the base station and rover receive differential GPS data and the baseline correction is solved between the two. This type of ground survey is accurate to 1.5 cm or less.

APPENDIX A

Project Narrative

Lower Columbia – Sandy Watershed

STARR
Strategic Alliance for Risk Reduction

LIST OF FIGURES

1. Introduction and Scope of Work

The Strategic Alliance for Risk Reduction (STARR), under Contract Number HSFEHQ-09-D-0370, task number HSFE10-10-J-00106 with the Federal Emergency Management Agency (FEMA) was scoped to acquire field survey for four streams in the Lower Columbia-Sandy Watershed (HUC 17080001).

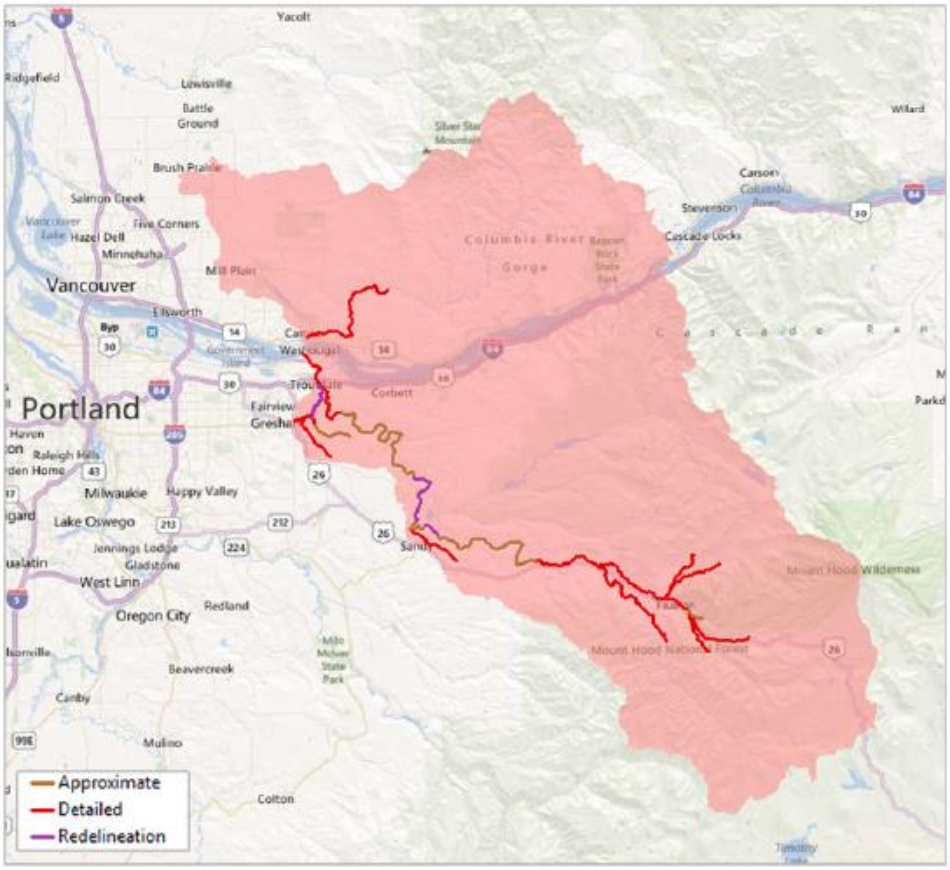

Figure 1: Study Area Map

The purpose of this survey is to provide current in channel elevations and structure information to be used in detailed analysis investigating the existence and the severity of flood hazards and revising the Flood Insurance Study (FIS) for Clackamas County OR, Multnomah County OR, and Clark County, WA.

2. Technical and Non-Technical Issues

There were limited technical issues primarily due to terrain and the inability to use GPS systems on much of the project area. This caused a substantial reduction in anticipated production during the data collection effort as well as the necessity to "think outside the box" and employ a number of different data collection techniques. Other items that affected production were the lack of physical access points to the project and the fact that the project access was fairly well limited to private property. There were also a substantial safety issues as a result of high water velocities and suspended sediment causing lack of visibility of the stream bed during the time of year the field surveys were performed. Specialized safety equipment was obtained based on the recommendation of the river rescue lead of the local fire department to mitigate some of these issues. During the course of the field surveys additional structures were noted and surveyed that had not been previously noted during the scoping of the project. It was noted that these structures were in areas of heavy tree canopy that obscured there visibility on the aerial photography used to establish the project scope. All survey work for this project was performed in accordance with FEMA Appendix M "Data Capture Standards" dated March 2009.

3. Information for Next Mapping Partner

3.1. Methodology

Surveying Methodology Overview

Approximately 60 structures and associated cross sections plus an additional 320 cross-sections were surveyed as part of this study. Surveying for this project included the following key points which will be discussed in detail later in this section:

- RTK and Static GPS with Robotic Total Stations – Established Primary & Secondary Survey Control along with conventional traverse for supplemental control.
- Sketches – Taped and Distance Meter Measurements in conjunction with sketches
- Photos – Upstream/Downstream Channel, Upstream/Downstream Bridge Face, and Overtopping Cross Section
- Data Collection – Data for cross sections and structure features was collected using Trimble Robotic Total Stations and electronic data collectors and a variety of other methods suitable for a project of this nature.

Static and Real Time Kinematic (RTK) GPS for Survey Control

Atkins used a combination of Trimble R8 GPS units with GNSS capabilities to perform both Static and RTK GPS in setting all survey control points on this project. The base network was established using a number of National Geodetic Survey (NGS) monuments as well as Oregon Department of Transportation (ODOT) control monuments. Atkins used this procedure to establish numerous primary points throughout the project area. Those primary points were then used as control checks for any subsequent GPS efforts. The NGS monuments used as the initial control checks when setting the primary control were as follows:

STATION	NORTH (ft)	EAST (ft)	Elev (ft)	COMMENTS
STAY	16286580.08	1686879.19	440.93	CORS PID DG5352
_CAP	16460875.40	1963097.88	3974.49	Fnd brass disk PID RC2011
8142	16485728.29	1825134.18	1005.63	Fnd brass disk PID AJ8142
AJ81	16493855.38	1828223.99	930.19	Fnd brass disk PID AJ8177
PDXA	16566018.86	1740410.62	59.50	ORDOT CORS STA http://www.theorgn.org/
WHEY	16486818.82	1888347.83	1062.83	Fnd brass disk PID RD4213
KENN	16475374.52	1911683.87	1427.27	Fnd brass disk PID AJ8181
GWN6	16637947.51	2067028.77	2475.56	CORS PID DJ6123
REDM	16083933.64	2125469.94	3088.43	CORS PID AH2507
CP20	16474080.27	1915091.45	1469.57	Fnd ODOT brass cap on conc Island ECC to PID RC1254
K389	16463835.40	1939938.09	2550.45	Fnd brass disc on top of rock PID RC1270
RD01	16493550.79	1830347.51	989.91	Fnd PK nail
PDXA	16566018.86	1740410.62	59.50	ODOT CORS STA http://www.theorgn.org/
ENGL	16580188.45	1764970.11	303.68	Fnd survey disk PID RD4327
POST	16547402.68	1796510.20	55.99	Fnd survey disk "POST RM1" PID RD0005
_G45	16559759.38	1809220.48	54.47	Fnd survey disk PID RD0116

COORDINATES : UTM ZONE 10 N
REF DATUM : NAD 83 (2007)
VERTICAL DATUM REFERENCE : NAVD 88
ORTHOMETRICS HEIGHTS : Derived from GRS80 Ellipsoid (6/27/12ADJ) and GEOID 09
Units : US Survey foot

All static control surveys were post-processed and adjusted using the Starnet® least squares adjustment software.

The Oregon Real-time GPS Network (ORGN) broadcast was used for real time corrections where available. Information regarding this system can be found at www.TheORGN.net

Supplemental Control where GPS was not Available
In a large number of instances GPS signals were not available due to either steep terrain or heavy vegetation and tree canopy. In these instances conventional traverses were run using Trimble S6 Robotic Total Stations with either Trimble TSC2 or TSC3 electronic data collectors. These traverses were based on the initial control established with GPS as noted above. All traverse were adjusted with a least squares adjustment using either Starnet® or Trimble Geomatics Office® software.

Structure Sketches and Measurements
Prior to collecting survey data with total stations shots on the structures and cross-sections, the structures were measured and sketched to determine what points would need to be located versus what measurements could be made with a tape or distance meter. Measurements were made at least twice to ensure accurate readings were recorded. Measurements made using tapes were confirmed against surveyed data points for correctness.

Photos

5

The required photos were taken for upstream & downstream channel, upstream & downstream face of structure, and the overtopping cross section. Several bridge or culvert faces for the project were difficult to photograph given the proximity of vegetation to the face of the structure or the depth of water in the river/creek. Photos which were difficult to capture the entire bridge or culvert were taken at an angled view from the banks. Photo stitching was conducted for photos with sufficient overlap and geometry to allow for that task. The photos were then renamed to associate them with the corresponding structure number.

Data Collection

Trimble S6 Robotic Total Stations with either Trimble TSC2 or TSC3 electronic data collectors were used to collect data on the features and cross sections for each bridge in the project area. The total station and associated backsight were setup over control points established in the Static and/or RTK methods previously described. At each setup a backsight control check was taken to ensure that the distance reading between the instrument and backsight agreed with the inversed distance based on the previously established coordinates for the points. Field Notes were kept regarding instrument and backsight numbers and heights for later QC versus the data collected in the handheld data collectors. Cross section data was also compared and confirmed against existing project LiDAR data where possible. The above methods were used for cross section data collection along the stream areas where possible as well. In some cases the stream cross sections were taken using a combination of GPS RTK methods combined with tape and hand level measurements. These areas were limited to locations where the terrain restricted the safe transport of other equipment.

Quality Control

- Field Notes vs. Raw Data – Positions, target heights, rod heights, and point description notes were compared between the data recorded in handheld data collectors versus notes kept in a field book.
- Control Checks – Check shots were utilized in both the GPS data collection and total station data collection to verify measured coordinates versus published or previously established coordinates.
- Photos – The photos were checked for coverage of required views as well as clarity.
- Sketches – The sketches were checked against the photos to ensure that all features required on each structure were either depicted in the sketch or the points.
- CAD Checks – The points were imported into AutoCAD to check point numbers as located versus point numbers labeled on sketches.
- LiDAR checks – The data was compared to the project LiDAR data as a check for vertical consistency.

4. References

FEMA Appendix M "Data Capture Standards" dated March 2009

Laser Noise

For any given target, laser noise is the breadth of the data cloud per laser return (i.e., last, first, etc.). Lower intensity surfaces (roads, rooftops, still/calm water) experience higher laser noise. The laser noise range for this survey was approximately 0.02 meters.

Relative Accuracy

Relative accuracy refers to the internal consistency of the data set - the ability to place a laser point in the same location over multiple flight lines, GPS conditions, and aircraft attitudes. Affected by system attitude offsets, scale, and GPS/IMU drift, internal consistency is measured as the divergence between points from different flight lines within an overlapping area. Divergence is most apparent when flight lines are opposing. When the LiDAR system is well calibrated, the line-to-line divergence is low (<10 cm).

Relative Accuracy Calibration Methodology

Manual System Calibration: Calibration procedures for each mission require solving geometric relationships that relate measured swath-to-swath deviations to misalignments of system attitude parameters. Corrected scale, pitch, roll and heading offsets were calculated and applied to resolve misalignments. The raw divergence between lines was computed after the manual calibration was completed and reported for each survey area.

Automated Attitude Calibration: All data were tested and calibrated using TerraMatch automated sampling routines. Ground points were classified for each individual flight line and used for line-to-line testing. System misalignment offsets (pitch, roll and heading) and scale were solved for each individual mission and applied to respective mission datasets. The data from each mission were then blended when imported together to form the entire area of interest.

Automated Z Calibration: Ground points per line were used to calculate the vertical divergence between lines caused by vertical GPS drift. Automated Z calibration was the final step employed for relative accuracy calibration.

Absolute Accuracy

The vertical accuracy of LiDAR data is described as the mean and standard deviation (sigma σ) of divergence of LiDAR point coordinates from RTK ground survey point coordinates. To provide a sense of the model predictive power of the dataset, the root mean square error (RMSE) for vertical accuracy is also provided. These statistics assume the error distributions for x, y, and z are normally distributed, thus we also consider the skew and kurtosis of distributions when evaluating error statistics.

APPENDIX C

LiDAR accuracy error sources and solutions:

Type of Error	Source	Post Processing Solution
GPS (Static/Kinematic)	Long Base Lines	None
	Poor Satellite Constellation	None
	Poor Antenna Visibility	Reduce Visibility Mask
Relative Accuracy	Poor System Calibration	Recalibrate IMU and sensor offsets/settings
	Inaccurate System	None
Laser Noise	Poor Laser Timing	None
	Poor Laser Reception	None
	Poor Laser Power	None
	Irregular Laser Shape	None

Operational measures taken to improve relative accuracy:

Low Flight Altitude: Terrain following is employed to maintain a constant above ground level (AGL). Laser horizontal errors are a function of flight altitude above ground (i.e., ~ 1/3000th AGL flight altitude).

Focus Laser Power at narrow beam footprint: A laser return must be received by the system above a power threshold to accurately record a measurement. The strength of the laser return is a function of laser emission power, laser footprint, flight altitude and the reflectivity of the target. While surface reflectivity cannot be controlled, laser power can be increased and low flight altitudes can be maintained.

Reduced Scan Angle: Edge-of-scan data can become inaccurate. The scan angle was reduced to a maximum of ±15^{o} from nadir, creating a narrow swath width and greatly reducing laser shadows from trees and buildings.

Quality GPS: Flights took place during optimal GPS conditions (e.g., 6 or more satellites and PDOP [Position Dilution of Precision] less than 3.0). Before each flight, the PDOP was determined for the survey day. During all flight times, a dual frequency DGPS base station recording at 1–second epochs was utilized and a maximum baseline length between the aircraft and the control points was less than 19 km (11.5 miles) at all times.

Ground Survey: Ground survey point accuracy (i.e. <1.5 cm RMSE) occurs during optimal PDOP ranges and targets a minimal baseline distance of 4 miles between GPS rover and base. Robust statistics are, in part, a function of sample size (n) and distribution. Ground survey RTK points are distributed to the extent possible throughout multiple flight lines and across the survey area.

50% Side-Lap (100% Overlap): Overlapping areas are optimized for relative accuracy testing. Laser shadowing is minimized to help increase target acquisition from multiple scan angles. Ideally, with a 50% side-lap, the most nadir portion of one flight line coincides with the edge (least nadir) portion of overlapping flight lines. A minimum of 50% side-lap with terrain-followed acquisition prevents data gaps.

Opposing Flight Lines: All overlapping flight lines are opposing. Pitch, roll and heading errors are amplified by a factor of two relative to the adjacent flight line(s), making misalignments easier to detect and resolve.